# p14 viral fusion protein driven cell-cell fusion induces micronuclei formation and a STING-dependent interferon response

By TETYANA MURDZA, B.Sc.

A Thesis Submitted to the School of Graduate Studies in Partial Fulfilment of the Requirements for the Degree Master of Science

## Descriptive Note

McMaster University MASTER OF SCIENCE (2021) Hamilton, Ontario (Department of Biochemistry and Biomedical Sciences)

TITLE: p14 viral fusion protein driven cell-cell fusion induces micronuclei formation and a STING-dependent interferon response.

AUTHOR: Tetyana Murdza, B.Sc.

SUPERVISOR: Dr. Karen Mossman

ADVISORY COMMITTEE: Dr. Matthew Miller and Dr. Ray Truant

PAGES: 58

## Lay Abstract

Viruses and their hosts continuously fight each other for survival. The host tries to protect itself from the virus by activating various features of its immune system, while the virus tries to block and evade detection by the immune system. One way that some viruses attempt to bypass the immune system and enhance spread involves expressing proteins that can merge together infected cells with neighboring uninfected cells. Cell-cell fusion disrupts the balanced environment within the cell, which is a form of stress that may activate immune responses. This work investigates if and how host cells may activate the immune system to respond and protect themselves from the cell merging activity of select viruses. We found that the stress associated with existing as a large, fused cell caused DNA damage and fragmentation. These DNA fragments could stimulate key immune sensors and initiate immune responses. We also observed an impaired ability of viruses to infect fused cells, but this restriction was not associated with typical immune responses, suggesting that some other biological change in fused cells created an environment that is not suitable for viral spread. Further investigation is required to fully understand this phenomenon; however, this study highlights some protective mechanisms of the host immune system in response to the stress of viral fusion protein induced cell-cell fusion.

## Abstract

The innate immune system is the first line of defence against viral infections. Conventionally, innate immune activation begins with the detection of foreign nucleic acids by pattern recognition receptors (PRRs), which triggers a signalling cascade that culminates in the production of interferon (IFN) and other inflammatory cytokines and chemokines. Over the past few years, a number of studies have shown that IFN innate immune responses can also be triggered by stressors, such as membrane perturbations, cytoskeletal perturbations, oxidative stress, and endoplasmic reticulum (ER) stress [1–3]. One way that some viruses provoke such stress responses is through membrane and cytoskeletal distortions during enveloped virus particle entry. In some cases, the glycoproteins responsible for virus particle entry can also trigger cell-cell fusion. The potential of cell-cell fusion to induce stress-based IFN responses analogous to those triggered by virus-cell fusion has not been addressed until very recently. To investigate if and how cell-cell fusion may induce antiviral mechanisms and IFN responses we used the reptilian reovirus p14 fusion associated small transmembrane (FAST) protein as a model of cell-cell fusion. We found that p14-mediated cell fusion led to the production of low level IFN and upregulation of interferon stimulated genes (ISGs) in a stimulator of interferon genes (STING) and interferon regulatory factor 3 (IRF3) dependent manner. We also observed that multinucleated cells experienced extensive DNA-damage that led to the accumulation of cytosolic DNA in the form of micronuclei. Micronuclei can be detected by cytosolic DNA PRRs like cyclic GMP-AMP synthase (cGAS) and signal IFN production through the cGAS-STING signalling axis. Additionally, early syncytia formation restricted replication of vesicular stomatitis virus (VSV), herpes simplex virus-1 (HSV), and vaccinia virus (VSV) in an IFN and IRF3 independent, and STING dependent manner, suggesting involvement of either a novel antiviral mechanism or suppression of virus replication and spread by biological changes in syncytial cells, such as cell cycle arrest. This study highlights a key role of DNA sensing pathways in the immune response to cell fusion associated stress and points out the importance of fusion kinetics in the selective advantage of syncytial viruses. Understanding the potential of syncytial cells to induce IFN responses and influence viral replication at a mechanistic level is beneficial to the design of improved oncolytic immunotherapy.

## Acknowledgements

Foremost, I would like to thank my supervisor Dr. Karen Mossman for giving me the opportunity to work and learn in her lab and for her continuous encouragement, guidance and support throughout the process of my Master's study and research. I would also like to thank my committee members, Dr. Ray Truant and Dr. Matthew Miller for their advice and suggestions that helped guide the course of the project.

Additionally, this work would not have been possible without the help of all our lab members. In particular, I would like to thank Susan Collins, Dr. David Hare, Dr. Arinjay Banerjee, Dr. Kaushal Baid, Dr. Maria Davola, and Dr. Wael Demian for sharing their vast knowledge and expertise. Their teachings helped me develop many of the skills I needed to complete this thesis and simply become a better scientist. I am very thankful to have spent these past two years working and chatting with such excellent mentors. We always had a fun time both in and outside the lab, which made the experience all the better.

Last but not least, I thank my parents Nataliya and Roman for their love and support through the ups and downs of this process.

# Table of Contents

## List of Figures

## List of Abbreviations and Symbols

| | |
|---|---|
| AIM2 | Absent In Melanoma 2, and interferon-inducible protein |
| ATM | Ataxia Telangiectasia Mutated |
| ATP | Adenosine Triphosphate |
| B18R | Soluble Interferon alpha/beta Receptor B18R |
| BSA | Bovine Serum Albumin |
| cGAMP | Cyclic Guanosine monophosphate-Adenosine Monophosphate |
| cGAS | Cyclic Guanosine monophosphate-Adenosine Monophosphate Synthase |
| CLR | C-type Lectin Receptor |
| CXCL10 | Chemokine interferon gamma-inducible protein 10 |
| DDR | DNA Damage Response |
| DDX4 | DEAD-Box Helicase 4 |
| DNA | Deoxyribonucleic acid |
| DNA-PK | DNA-dependent Protein Kinase |
| dsDNA | Double stranded deoxyribonucleic acid |
| dsRNA | Double stranded ribonucleic acid |
| EDTA | Ethylenediamine tetraacetic acid |
| EGFR | Epidermal Growth Factor Receptor |
| ER | Endoplasmic Reticulum |
| FBS | Fetal Bovine Serum |
| GAPDH | Glyceraldehyde 3-phosphate dehydrogenase |
| GECI | Genetically Encoded Calcium Indicator |
| GFP | Green Fluorescent Protein |
| GMP-AMP | Guanosine Monophosphate-Adenosine Monophosphate |
| GTP | Guanosine Triphosphate |
| H2AX | H2A histone family member X |
| HIV | Human Immunodeficiency Virus |
| FAST | Fusion Associated Small Transmembrane |
| HR | Homologous Recombination |
| HRSV | Human Respiratory Syncytial Virus |
| HSV | Herpes Simplex Virus |
| IFI16 | Interferon-inducible myeloid differentiation transcriptional activator (Gamma-interferon inducible protein IFI16) |
| IFIT1 | Interferon Induced Protein with Tetratricopeptide Repeats 1 |
| IFN | Interferon |
| IFNAR | Interferon α/β Receptor |
| IKK | Inhibitor of KappaB Kinase |
| IRE1α | Inositol-Requiring Enzyme 1-alpha |
| IRF | Interferon Regulatory Factor |

| | |
|---|---|
| ISG | Interferon Stimulated Gene |
| ISGF3 | Interferon Stimulated Gene Factor 3 |
| MDA5 | Melanoma Differentiation-Associated Protein 5 |
| MDC1 | Mediator of DNA damage Checkpoint Protein 1 |
| MeV | Measles Virus |
| MRN | MRE11, RAD50 and NBN complex |
| NF-κB | Nuclear Factor kappa B |
| NHEJ | Non-homologous End Joining |
| NLR | NOD-like Receptors |
| OAS1 | 2'-5'-Oligoadenylate Synthetase 1 |
| PAMPs | Pathogen Associated Molecular Patterns |
| PBS | Phosphate Buffered Saline |
| PKR | Protein Kinase R |
| PRR | Pattern Recognition Receptor |
| RIG-I | Retinoic acid-inducible gene I |
| RLR | Retinoic acid-inducible gene I-Like Receptor |
| RNA | Ribonucleic Acid |
| ROS | Reactive Oxygen Species |
| RT-qPCR | Reverse Transcriptase Quantitative Polymerase Chain Reaction |
| SARS-CoV-2 | Severe Acute Respiratory Syndrome Coronavirus 2 |
| SASP | Senescence-Associated Secretory Phenotype |
| SeV | Sendai Virus |
| SKIV2L | Ski2 Like RNA Helicase |
| SMC1 | Structural Maintenance of Chromosome Protein 1 |
| ssDNA | Single-stranded Deoxyribonucleic Acid |
| ssRNA | Single-stranded Ribonucleic Acid |
| STAT | Signal Transducer and Activator of Transcription |
| STIM1 | Stromal Interaction Molecule 1 |
| STING | Stimulator of Interferon Genes |
| TBK1 | TANK-binding Kinase 1 |
| THF | Telomerase life-extended Fibroblasts |
| TLR | Toll-like Receptor |
| TMPRSS2 | Transmembrane Serine Protease 2 |
| TREX1 | Three Prime Repair Exonuclease 1 |
| UPR | Unfolded Protein Response |
| UV | Ultraviolet |
| VacV | Vaccinia Virus |
| VSV | Vesicular Stomatitis Virus |

# Introduction

## The Innate Immune Response

Humans are routinely exposed to millions of pathogens in their environment and the immune system serves to protect against these invaders. The adaptive immune system applies robust, pathogen specific responses to clear an infection; however, this response is slow to develop upon exposure to a new pathogen. Without additional protective measures, this time delay would allow a pathogen to replicate and cause extensive damage to the host. Thus, the innate immune system faces the task of protecting the host during the first few critical days of infection. The innate immune system detects conserved features of pathogens that are absent in the host, referred to as pathogen-associated molecular patterns (PAMPs), and quickly initiates an inflammatory response to help clear the invader[4].

Pattern recognition receptors (PRRs) are located in various compartments of the cells and detect PAMPs such as glycans, nucleic acids, and proteins[5]. For instance, formylmethionine-containing peptides are unique to prokaryotes and can be identified by the innate immune system as a bacterial infection[4]. Additionally, outer surface molecules of many microorganisms such as the peptidoglycan cell wall and flagella of bacteria, as well as lipopolysaccharide (LPS) on Gram-negative bacteria and teichoic acids on Gram-positive bacteria do not occur in their multicellular hosts, making these molecules effective immunostimulants[4]. Double-stranded RNA is one of the most common PAMPs in the detection of viral infections[4].

There are four main types of PRRs: Toll-like receptors (TLRs); retinoic acid-inducible gene I (RIG-I)-like receptors (RLRs); nucleotide-binding oligomerization domain-like receptors (NLRs); and C-type lectin receptors (CLRs) [5]. TLRs are found on the cell or endosomal membrane and recognize a wide range of PAMPs including lipids, lipoproteins, proteins, glycans, and nucleic acids [5]. RLRs and NLRs serve as a cytosolic detection system, with RLRs like RIG-I and MDA5, recognizing viral RNA and NLRs recognizing viral and bacterial DNA, as well as other bacterial PAMPs through the assembly of inflammasomes[5]. CLRs are transmembrane proteins located at the cell membrane, which recognize glycans[5]. Depending on the type of PRR activated varying signalling cascades are initiated leading to the production of interferons (IFN) and other pro-inflammatory cytokines in the infected cells [5–7].

Although downstream signalling cascades vary depending on the type of PRR activated, they all generally involve the activation of key transcription factors: namely, interferon regulatory factor 3 (IRF3), IRF7 and NF-κB, which induce transcription of IFN [8]. Type I IFNs are the principal cytokines involved in the antiviral response, and they include IFN-α, IFN-β, as well as several other isoforms [6,7,9]. All nucleated cells can respond to viral infection by inducing type I IFN, whereas type II IFN (IFN-γ) are exclusively produced by T cells and NK cells [6]. Type III IFN (IFN-λ) resemble type I IFN in mechanism of action, although they target different receptors [10]. Interferons are produced in infected cells and can protect neighbouring cells by

binding to IFN receptors (IFNAR) and initiating the activation of the ISGF3 transcription factor complex, composed of STAT1, STAT2, and IRF9 [9]. The activated ISGF3 complex induces expression of a specific subset of interferon stimulated genes (ISGs), whose protein products mediate the antiviral, immunostimulatory, and antiproliferative effects of these cytokines [7,9].

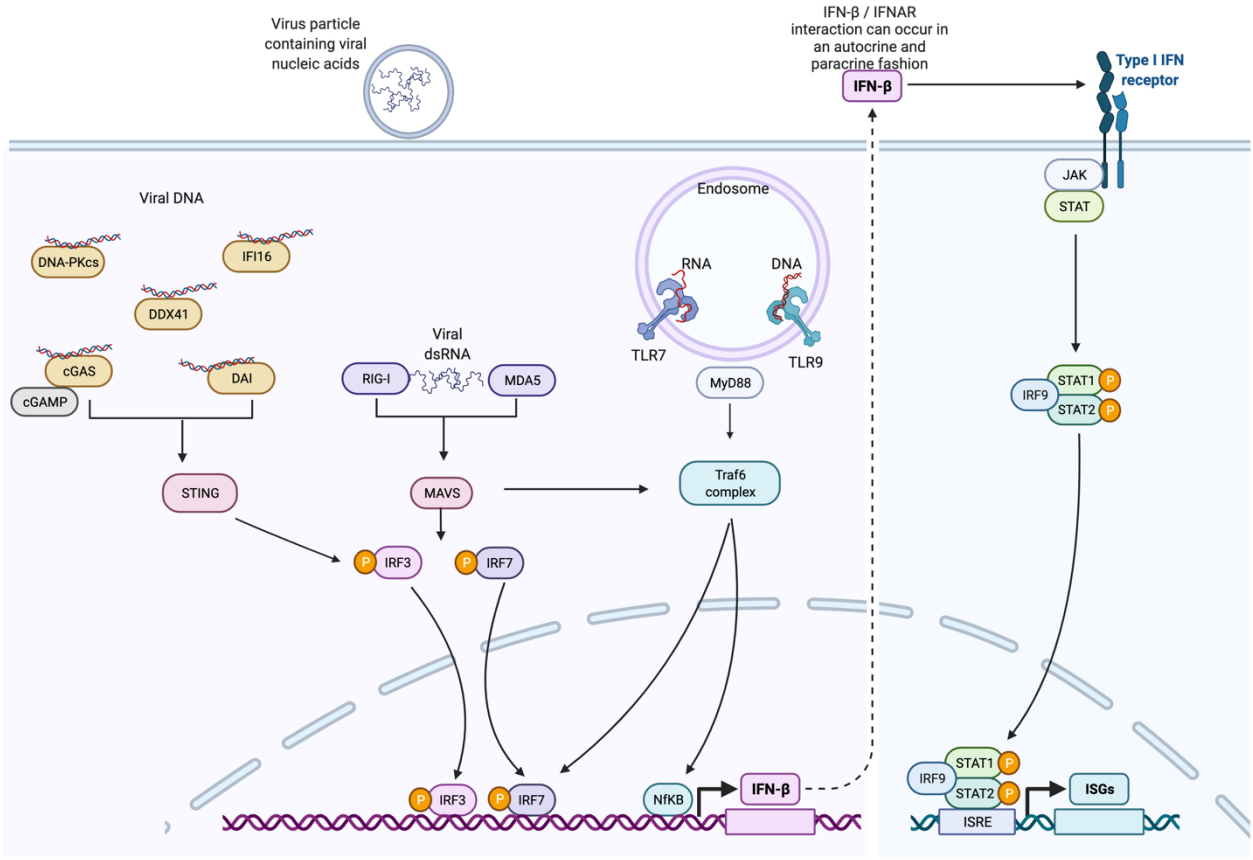


**Figure 1**. Schematic of key signalling pathways of the innate immune response. Created with BioRender.com. Viral nucleic acids can be detected by DNA and RNA sensors in the cytoplasm or endosome. Foreign nucleic acid sensing results in the activation of key transcription factors like IRF3 and IRF7, which drive the production of IFN. IFN can bind IFNAR receptors in an autocrine or paracrine manner and stimulate the upregulation of ISGs through the JAK/STAT signalling axis.

## The cGAS-STING axis

Cyclic GMP-AMP (cGAMP) synthase (cGAS) is an important cytosolic PRR of the innate immune system. Upon sensing of cytosolic double-stranded DNA (dsDNA), cGAS produces the second messenger cGAMP. cGAS is activated by dsDNA and single-stranded DNA that can form internal duplex structures in a sequence independent but length dependent manner[11]. While cGAS can also bind dsRNA, this does not trigger the conformational change required to activate cGAS[12]. The structural rearrangement in cGAS exposes the catalytic pocket to enable cGAS to catalyze the synthesis of 2'3'-cyclic GMP-AMP (cGAMP) from ATP and GTP substrates[13].

cGAMP acts as a second messenger to activate the adaptor STING, a transmembrane protein anchored to the endoplasmic reticulum (ER) through interaction with the $Ca^{2+}$ sensor stromal interaction molecule 1 (STIM1)[14,15]. Upon cGAMP binding at the STING ligand binding pocket, STING oligomerizes into a tetramer and translocates from the ER to the Golgi apparatus, where STING is palmitoylated at two cysteine residues[12]. Subsequently, STING recruits the kinase TBK1, which phosphorylates STING at the C-terminal domains, allowing STING to recruit IRF3, which is also phosphorylated by TBK1. IRF3 then dimerizes and traffics to the nucleus. STING also activates the kinase IKK, resulting in the activation and nuclear translocation of NF-κB, where it works with IRF3 and other transcription factors to induce expression of IFN and other proinflammatory cytokines[12]. cGAMP can also alert uninfected neighbouring cells to activate interferon pathways directly by passing across gap junctions, a useful mechanism for combatting viruses that antagonize immune responses[16].

In addition to mediating protective immune defenses, the cGAS-STING pathway also detects tumor-derived DNA generating intrinsic antitumor immunity, and in the case of aberrant activation can lead to autoimmune and inflammatory disease[12]. Tight regulation of this pathway is important for preventing excessive immune activation from self-DNA recognition.

## Non-canonical roles of STING

While the most well-known function of STING is its role in stimulating IFN responses via the cGAS-STING signalling pathway, additional roles of STING in autophagy, cellular senescence, and protein translation inhibition have also been reported. STING signaling has been shown to promote cancer cell clearance by autophagy, necrosis, or apoptosis independently of IRF3 and NF-κB transcriptional activation, suggesting that pathways other than IFN responses can be activated downstream of STING[17].

Additionally, STING has been implicated in stress-induced innate immune responses. IFN responses to calcium associated ER stress depend on STING and TBK1[2]. STING was also required for an IFN response to membrane perturbations by virus-like particle entry and was shown to translocate from the ER to cytoplasmic punctate structures, a hallmark of STING activation [3,18]. In neural stem/progenitor cells acute oxidative stress caused disruptions to the

maturation of nuclear lamina and release of chromatin fragments activating the cGAS-STING-IFN response[19].

How STING modulates its various effects is largely unclear. One regulatory mechanism involves EGFR mediated tyrosine phosphorylation of STING which dictates whether STING traffics to endosomes, inducing IFN responses, or moves to autophagosomes and shifts to autophagy[20]. A region of STING unique from domains involved in IFN signalling called the unfolded protein response (UPR) motif was recently shown to mediate calcium homeostasis, ER stress and T cell survival[21]. Additionally, reactive oxygen species can oxidize the Cysteine 147 residue of STING which prevents STING polymerization and downstream activation of IFN responses, and may hence promote initiation of alternative pathways like cell death[22].

## Discriminating self from non-self nucleic acids

The induction of type I interferon is predominantly initiated by sensing of foreign nucleic acids. Distinguishing foreign nucleic acid from self nucleic acid is a crucial element to managing proper function of the IFN response. Three major factors aid in making this distinction: the availability (as determined by the local concentration, rate of degradation by nucleases and level of shielding), the localization, and the structure of the nucleic acids[23].

Generally, self nucleic acid is rapidly degraded by nucleases before it can be sensed by nucleic acid receptors. Following an unfolded protein response (UPR), OAS1-activated RNaseL and IRE1α cleave endogenous RNA, forming RNA fragments that can serve as ligands for RLRs; however, the SKIV2L RNA exosome degrades this endogenous RNA[24]. DNase I degrades cell-death derived DNA and DNA accumulated in the cytosol of phagocytic cells, lysosomal DNase II degrades phagocytosed DNA and clears nuclear DNA that enters the autophagy pathway, and TREX1 degrades cytosolic DNA[25].

Endogenous DNA is largely confined within compartments like the nucleus and mitochondria, thus the mere presence of DNA in the cytoplasm activates PRRs like cGAS, AIM2, IFI16 and DDX4[23]. Interestingly a large fraction of cGAS is associated with chromatin during mitosis, but is not activated due to its hyperphosphorylation and chromatin tethering which prevents the oligomerization required for cGAS activity[26]. Thus, during cell division cGAS is chromosome-tethered and lacks the ability to sense self-DNA and activate immune responses. In the endolysosomal compartment, TRR9 is the dominant sensor of foreign DNA[27]. TLR9 preferentially detects DNA containing CpG dinucleotides, which are much less common in eukaryotic self DNA compared to bacterial DNA[5,27]. Modifications to endogenous DNA can impact DNA sensing. For instance, oxidative stress results in the incorporation of oxidative adducts- commonly 8-hydroxyguanosine (8-OHG)- which stabilizes the DNA against TREX1 exonuclease degradation[28]. This ultimately leads to the accumulation of cytosolic DNA and cGAS activation.

Distinguishing self and non-self RNA is more complex, as both can be found within the same compartments of a cell. RNA sensing PRRs like RIG-I, MDA5, PKR, OAS1 and TLR3

recognize long double stranded RNA, a hallmark of RNA and DNA virus replication, or ssRNA with secondary structures[29,30]. Various modifications of RNA help mediate the differentiation between self and non-self RNA. RIG-I is activated by blunt-end 5'-triphosphate dsRNA, and to a lesser extent 5'-diphosphate RNA[31,32]. IFIT1, IFIT5 and PKR have also all been shown to recognize 5'-triphosphorylated ssRNA[33]. Presence of RNA with 5'-triphosphate ends in the cytosol is indicative of a viral infection, as the RNA must have formed outside the nucleus. Endogenous RNA is processed before leaving the nucleus by backbone or base modifications, splicing and 5'capping, which results in the removal of 5'triphosphate ends. 2'-O-methylation, a component of 5' capping of RNA in eukaryotes serves to prevent sensing of self RNA, as it abolishes recognition of self RNA by RIG-I and IFIT1[31,34,35]. However, some flaviviruses, coronaviruses, paramyxoviruses and rhabdoviruses, reoviruses, and pox viruses have evolved mechanisms to disguise their RNA molecules as self RNA by encoding 2'-O-methyltransferases, effectively evading innate immune activation[36].

## DNA damage repair and its impact on DNA-sensing innate immune signaling pathways

Eukaryotic cells are frequently exposed to stressors, both exogenous (toxic drugs, UV irradiation) and endogenous (DNA replication stress, topoisomerase poisons). Genotoxic stress can result in chromosome missegregation and fragmentation and the formation of micronuclei in the cytoplasm. To prevent malignant transformation or immune damage, cells have evolved elaborate mechanisms to repair damaged DNA. There are two major mechanisms of DNA damage repair. The first is homologous recombination (HR), which is a high fidelity repair pathway that occurs during late S and G2 phases of the cell cycle[37]. HR initiates when the MRE11-RAD50-NSB1 (MRN) complex detects double-stranded breaks, which induces the autophosphorylation of Ataxia-telangiectasia mutated (ATM). ATM recruits phosphorylated H2AX checkpoint kinase, cohesion protein SMC1, and binds to the mediator protein MDC1[38]. P53-binding protein 1, breast cancer type 1/2 and additional MRN complex are recruited to the damaged site, completing the homologous recombination repair[39]. The second repair mechanism is non-homologous end-joining (NHEJ), which occurs during all cell cycle phases and repairs DNA junctions containing mutations. The Ku70-Ku80 heterodimer recognizes a damaged site, and along with the DNA-dependent protein kinase catalytic subunit promotes the recruitment of other NHEJ proteins to complete the repair[37].

Despite the cell's efforts at repairing and shielding damaged DNA from PRRs of the innate immune system, several DNA sensors have been shown to recognize and bind damaged endogenous DNA. cGAS was recently identified as an important cytosolic DNA sensor that can recognize and bind damaged DNA[17,40]. cGAS is recruited to micronuclei following DNA damage and nuclear envelope rupture; however, direct evidence of cGAS activation is lacking as is an understanding of what form of chromatin DNA is detected in micronuclei[41,42]. Other DNA sensors present in the cell capable of sensing damaged DNA include DAI and RNA polymerase III[43].

Interestingly, multiple proteins of the DNA damage repair pathway have been associated with mediators of the interferon response pathway. The DNA-dependent protein kinase (DNA-PK) complex, consisting of Ku70, Ku 80, and its catalytic subunits, has been shown to phosphorylate IRF3, promoting nuclear retention of IRF3[44]. Additionally, DNA-PK has been proposed to act as a PRR upstream of STING by binding cytoplasmic DNA and triggering IFN and cytokine production in and IRF3-dependent manner[45].

The degree of inflammatory gene induction by genomic DNA damage is usually lower than that induced by DNA transfection or viral infection[17]. The extensive DNA repair mechanisms of the cell are likely a prime contributing factor for these differences. Deficiencies in DNA damage repair components can exacerbate autoinflammatory disease and tumorigenesis[37].

## Viral Glycoproteins and the Syncytial Phenotype

All viruses contain genetic material (DNA or RNA) encased in a protein shell called a capsid[46]. Enveloped viruses have an additional membrane surrounding the capsid, composed of lipids, viral glycoproteins, and some host proteins[46]. Viral fusion proteins have been broadly categorized into four classes depending on the conformational structure and mechanism used for fusion of the viral envelope with the cell membranes: class I, with a characteristic α-helix trimer (as in HIV-1 transmembrane gp41); class II, with a β-sheet-based elongated ectodomain (as in dengue virus glycoprotein); class III, composed of an α-helix and β-sheet combined ectodomain (as in rabies virus G glycoprotein) and class IV, composed of the FAST protein family of some non-enveloped Reoviruses[47].

These glycoproteins assist virion entry into a host by catalyzing envelope fusion directly at the cell membrane or with endosomal membranes[48]. The location of fusion varies across viral families, cell types, and depends on the triggering mechanism required for activation. Enveloped virus fusion proteins are maintained in a pre-fusion conformation by suppressors in one of the fusion protein domains or in a different viral glycoprotein[48]. Activation of the fusion capability requires priming (often by a proteolytic cleavage), followed by triggering of a conformational change in the fusion protein[48]. Viral fusion proteins are typically triggered through interaction with a cell surface receptor, proton binding to the fusion protein at low pH, or a combination of these two events.[48] The triggered conformational change is usually irreversible, allowing the protein to only act once before losing the capacity to mediate fusion with a subsequently presented membrane[48].

Some viruses have evolved the ability to trigger cell-cell fusion between infected and neighbouring cells. Apart from the Orthoreovirus and Aquareovirsus subfamilies of *Reoviridae*, syncytial viruses are enveloped, and their envelope fusion glycoproteins are the primary initiators of cell-cell fusion. Evidence of syncytia formation has been documented for viruses of the *Herpesviridae, Paramyxoviridae, Coronaviridae and Retroviridae* families[47].

Herpesviruses are large and diverse double stranded DNA viruses capable of establishing long-life persistent infections. Presence of multinucleate cells in skin lesions and in the lower respiratory tract have been identified as hallmarks of Herpesvirus infection[49,50]. However, the degree of cell-cell fusion among clinical isolates and laboratory strains vary in vitro, and the significance of syncytia formation for viral replication and spreading in vivo remains unclear[51,52]. In herpesviruses, the mechanism of cell-cell fusion is poorly understood and cell type specific, but does require the glycoprotein gB homodimer gH/gL heterodimer fusion complex[53,54]. In particular, mutations or truncations in the gB glycoprotein can yield pronounced syncytia formation in vitro[55,56].

Paramyxoviruses are negative-strand RNA viruses, and some are capable of inducing cell-cell fusion: Sendai, Nipah, Hendra, Measles (MV) and human respiratory syncytial virus (HRSV)[47]. Multinucleated cells have been observed in lymph nodes, respiratory tracts and thymus of MV infected patients and in vivo, infected syncytia are capable of producing infectious virus particles[57,58]. Syncytia are a hallmark cytopathic effect of HRSV, which infects superficial airways and type I alveolar epithelial cells and causes infant lower respiratory tract diseases [59]. Measles virus (MV) relies on cooperative activity between the hemagglutinin protein (HA) and the fusion protein (F) for membrane fusion[60]. HA recognizes receptors on the target membrane and induces conformational changes in the F protein, which allows F to insert the fusion peptide into the target membrane, allowing for pH-independent fusion[61]. The fusion ability of HRSV is also largely dependent on F, although the details of the fusion mechanism are still debated[47].

Coronaviruses are positive single-stranded RNA viruses that have been at the forefront of the prior global outbreaks of Severe Acute Respiratory Syndrome Coronavirus (SARS-CoV) in 2001, Middle Eastern Respiratory Syndrome Coronavirus (MERS-CoV) in 2012, and the current COVID-19 pandemic driven by SARS-CoV-2. Lung tissue of patients with severe respiratory disease displayed evidence of large infected syncytia, and the syncytial phenotype has also been recapitulated in vitro systems[62–64]. The spike protein (S) responsible for coronavirus entry is driving cell-cell fusion in CoV infections, with the S1 N-terminal domain mediating receptor binding and the S2 C-terminal domain driving membrane fusion[65]. In the case of SARS-CoV-2 spike, interaction between the spike fusion protein and the ACE2 host receptor activates TMEM16F, triggering the unsheathing of the S2 fusion active domain of spike, leading to membrane fusion and syncytia formation[64].

Retroviruses are positive single-stranded RNA viruses whose genomes are reverse transcribed into proviral DNA, which is subsequently integrated into the host cell genome. The human immunodeficiency virus (HIV) and the human T-lymphotropic virus (HTLV) can induce cell-cell fusion in vitro; however, only HIV infection has been seen to cause T-cell, macrophage and dendritic cell syncytia formation in vivo[66–68]. Syncytia in patient samples were much smaller than those observed in vitro models.

While viral fusion proteins are essential to drive cell-cell fusion, endogenous cellular proteins may also play vital roles. The small GTPase RhoA was essential for HRSV-mediated

syncytia formation through modulation of microvilli at the cell surface[69]. Additionally, the TMPRSS2 cellular protease primes and activates the S protein of SARS-CoV-2.[70] A requirement for intrinsic cellular machinery may explain why the cell-cell fusion ability of many syncytial viruses varies among cell types.

## Fusion Associated Small Transmembrane (FAST) Proteins

FAST proteins are a unique class of viral fusion proteins expressed by non-enveloped reoviruses of the *Orthoreovirus* and *Auquareovirus* genera. FAST proteins are the smallest viral fusogens (95-198 residues) and are not involved in virus entry like fusion proteins of enveloped viruses; they exclusively mediate cell-cell fusion and syncytia formation independently of specific receptor recognition[71]. Structurally, FAST proteins are single pass transmembrane proteins with a small ectodomain (19-37 residues) and longer endodomain (36-141 residues). All three domains work co-operatively to drive the fusion process. When FAST proteins are expressed in cells, they traffic through the endoplasmic reticulum (ER)-Golgi pathway to the cell membrane, where they accumulate and form multimeric complexes. Translation initiation from suboptimal codons and excessive degradation by the ER-associated degradation pathway delays arrival of FAST proteins at the plasma membrane, thereby synchronizing syncytium formation with the replication cycle of the virus.

The fusion mechanism of FAST proteins differs from that of envelope virus fusogens, while maintaining some degree of similarity. There are three distinct stages of FAST protein mediated cell-cell fusion. First is the pre-fusion stage, where FAST proteins rely on surrogate cellular adhesion machinery at adherens junctions, such as calcium-dependent cadherin proteins, to mediate cell-cell attachment[72]. This allows for membrane approach as the FAST protein ecodomains are too short to span the intercellular gap between adjacent cells. In contrast, enveloped virus fusogens use conformational changes in the fusion protein to drive membrane apposition. The second stage involves membrane merger, where shallow insertion of the FAST protein into the outer leaflet of the membrane bilayer induces membrane curvature, generating a hemifusion intermediate. The transmembrane and endodomains work cooperatively to promote pore formation. Finally post-fusion occurs, where rearrangements in the cortical actin cytoskeleton allow for pore expansion and syncytia formation. Annexin 1 and the FAST protein C-terminal endodomain are required for effective pore expansion during these post-fusion events[73].

Fusogenic reovirus infections are more pathogenic than their non-fusogenic counterparts as they can induce meningo-encephalomyelitis, pneumonia, neurological dysfunction and enteric syndrome. Several cases of acute respiratory tract infection and meningo-encephalitis in humans have been associated with Orthoreoviruses of bat origin, suggesting that these viruses could emerge as zoonotic infections[74–78]. Therefore, it would be beneficial to better understand how FAST protein driven cell fusion impacts pathogenesis of these viruses and whether the host immune system is primed to respond to such fusion events.

**Cell-cell fusion associated innate immune responses**

As aforementioned, several viruses have been observed to cause syncytia formation among host cells as part of their cytopathic effect. In addition to the syncytial HRSV, HIV, MeV and HSV viruses, some bacterial pathogens like *Mycobacterium tuberculosis* and the melioidosis causing bacteria *Burkholderia pseudomallei* also produce syncytia upon infection[42,79]. The ability of a pathogen to fuse host cells has been proposed as advantageous for cell-to-cell spread of the pathogen, while evading detection by the adaptive immune system. However, despite the enhanced cytopathic effect or syncytial viruses, some cases have been documented where a syncytial phenotype was not beneficial to the virus. While syncytial variants of HSV and HIV outcompete their non-syncytial counterparts in vitro, they display restricted replication in vivo[80,81]. Additionally, fusogenic adenovirus replicated efficiently at a high multiplicity of infection (MOI), but at lower MOI virus replication was impaired and restricted to a single nucleus within the syncytial cell[82]. This suggests that some innate immune host response may counteract the detrimental effects of syncytia formation.

Cell-cell fusion involves extensive membrane and cytoskeletal disruption and reorganization, processes which have been proposed as stress-based triggers of IFN responses [1,83–85]. Membrane perturbations have been studied using a broad range of inactivated viruses and virus-like particles lacking the viral genome and capsid. All these studies demonstrated that enveloped virus particle entry could induce a subset of ISGs through IRF3 activation independently of PRRs (specifically TLRs and RLRs) [86–89]. Additionally, p14 reptilian reovirus FAST protein lipoplex fusion was sufficient to induce an IRF3 dependent antiviral response, while fusion incompetent p14 failed to provide antiviral protection [90]. Initial findings proposed that the antiviral response to p14 lipoplexes was IRF3 dependent and IFN independent; however, recent work with IFNAR knock-out cells highlighted that low level IFN is still required for antiviral responses in circumstances where IFN is difficult to detect by conventional assays[90,91]. Thus, while de novo IFN may not be required for the antiviral response to virus-like particles and p14 lipoplexes, constitutive or low level IFN may play a role. With the added resources of IFNAR knock-out cells and B18R IFN blockade, we can re-address previous observations to better understand the complexities of innate immune responses. Additionally, the IFN response to p14 FAST protein lipoplexes was dependent on the RLRs RIG-I and MDA5 even though no external nucleic acids were introduced[92]. A study by Holm *et al*. also showed that the IFN response to HSV virus-like particles lacking the viral genome required STING[3]. These studies point towards a role for nucleic acid sensors in IFN responses to membrane perturbations. Whether these nucleic acid sensors are activated by endogenous nucleic acids, or some other means warrants further investigation.

Despite the growing body of evidence of stress-based IFN responses, the mechanisms of how these various stressors are communicated to downstream effectors remain unclear. In particular, researchers have only recently begun addressing cellular responses to cell-cell fusion and any potential associated IFN signalling, thus very little is known about this process[42]. We

hypothesized that cell-cell fusion mediated by the p14 FAST protein can trigger IFN responses analogous to those induced by external p14 lipoplex fusion and serve as one aspect of the host defence mechanism against syncytial viruses. To address this hypothesis, we engineered cells that can be induced to express p14, creating a simple system that allows us to study the consequences of cell-cell fusion in the absence of the added PAMPs found in full syncytial viruses. We monitored the production of IFN and ISGs following cell fusion and addressed the involvement of key signalling molecules by monitoring these IFN responses in the appropriate knock-out cell types.

# Materials and Methods

## Generation of Cell Lines

Cell lines expressing p14 under a tetracycline inducible promoter were generated using a PiggyBac vector system, which introduces a gene of interest into the cell genome through transposon recombination [93]. The cDNA sequence of the p14 FAST protein was amplified by PCR using the following forward primer:
GGGGACAAGTTTGTACAAAAAAGCAGGCTTCACCATGGGGAGTGGACCCTCT, and reverse primer:
GGGGACCACTTTGTACAAGAAAGCTGGGTCCTAAATGGCTGAGACATTATCGATGTTG. These primers introduced recombination sequences flagging the 5' and 3' ends of the gene, which allowed the p14 gene to be introduced into the PB-TAG vector under an inducible promoter by a two-step recombination reaction mediated by BP and LR clonase enzymes.

Three plasmids: PB-TAG (encoding the gene of interest), pCYL43 (encoding the PBase recombination enzyme), and PB-CAG rtTA (encoding the rtTA protein which initiates gene expression in the presence of doxycycline) were nucleofected into telomerase life-extended human fibroblasts (THF) [94,95]. p14 positive cells were selected for with 3μg/mL puromycin. Additionally, the p14-THF cell line was cultured from a single cell clone. p14-THF IRF3$^{-/-}$ and p14-THF STING$^{-/-}$ cells were generated in the same manner, but plasmids were inserted into the appropriate THF knock-out cell type rather than wild type THFs.

To generate the IFN-GFP reporter p14-THF cells, p14-THF cells were transduced with IFN-GFP reporter lentivirus, transfected with 1μg/mL Poly:IC using lipofectamine 3000, and harvested in FACS buffer (PBS, 1% BSA, 5mM EDTA). The GFP positive population was sorted on a Beckman Coulter MoFlo XDP and collected for subsequent experiments.

## Quantitative RT-qPCR

RNA was extracted from cells homogenized in TRIzol reagent (Invitrogen). cDNA was subsequently prepared from 500 ng of RNA using the iScript cDNA Synthesis Kit (BioRad). Quantitative PCR reactions containing TaqMan probes and TaqMan Universal PCR Master Mix (Applied Biosystems) were prepared as per the manufacturer's instructions and run on a StepOnePlus Q-PCR instrument (Applied Biosystems). ΔΔCt values were calculated from instrument generated Ct values, using GAPDH as an endogenous control. Changes in gene expression were represented in terms of fold change relative to mock (calculated as $2^{-\Delta\Delta Ct}$). Taqman probes for human GAPDH (Hs02758991_g1), IFIT1 (Hs03027069_s1), and CXCL10 (Hs00171042_m1) were used. Transcript levels of p14 were probed SsoFAST EvaGreen Supermix and custom designed primers (*p14 FDW*: TTAGCGTTTGGCTTCTGGTT; *p14 REV:* GGCTCGTATGGGTCTTCGTA; *GAPDH FWD*: GGAGCGAGATCCCTCCAAAAT *GAPDH REV*: GGCTGTTGTCATACTTCTCATGG).

Significant differences in the data were calculated by one-way ANOVA or two-way ANOVA tests as required.

**VSV-GFP Plaque Reduction Assay**

Cells were pre-treated with 0.01μg/mL doxycycline for 6 hours, then challenged with VSV-GFP, or doxycycline was added immediately following the 1 hour VSV-GFP infection. As a positive control, cells were pre-treated with 20 μg/mL of Poly I:C. Supernatants were transferred onto fresh THF-IRF3 knock-out cells and incubated for 8 hours prior to infection to test for IFN production. F11 overlay media containing 2% FBS and 1% methylcellulose was added to restrict plaques. Green fluorescence from VSV-GPF was measured using a Typhoon laser scanner (GE Healthcare) 20 hours post infection. GFP fluorescence intensity was quantified using ImageQuant software and each condition was normalized relative to mock infected cells. HSV-GFP and VacV-GFP infections were also done in this manner. Significant differences in the data were calculated by one-way ANOVA or two-way ANOVA tests as required.

**Immunofluorescence**

Cells were seeded on coverslips and treated with 0.01 μg/mL doxycycline for up to 48 hours. Poly I:C or virus treatment was applied as a positive control for innate immune sensor activation. Post-treatment, cells were fixed with formalin for 10 minutes at room temperature, washed three times in PBS, and permeabilized with 0.2% Triton X-100 in PBS for 10 minutes at room temperature. The cells were once again washed three times with PBS and blocked with 3% BSA, 3% goat serum, 0.2% Tween-20 in PBS overnight. The samples were then incubated with primary antibody for 1 hour, washed, and incubated with secondary antibody (AlexaFluor488 diluted 1:400 in blocking buffer) for 1 hour. Cells were subsequently stained with CellMask Deep Red plasma membrane stain 1:10000 in PBS for 10 minutes. Coverslips were mounted onto slides with ProLong Gold antifade reagent with DAPI and left to cure overnight at room temperature. Images were acquired on a Zeiss Axio Imager M2 or EVOS FL Auto 2 widefield microscope at 20X magnification.

**Flow Cytometry**

IFN-GFP p14-THF cells were treated with 0.01 μg/mL doxycycline for 24 and 40 hours. As a positive control, cells were infected with 2 pfu of Sendai virus for 24 hours. Cells were harvested in FACS buffer (PBS, 1% BSA, 5mM EDTA) and analysed on a BC CytoFlex analyser. p14-THF cells that did not contain the GFP reporter cassette were used to set the negative gate.

**Western Blot**

Cell lysates were harvested in lysis buffer containing 50 mM HEPES pH 7.4, 150mM NaCl, 1% Triton-X, 10% glycerol, 1.5 mM $MgCl_2$, 1 mM EGTA with 100μM aprotinin, leupeptin, pepstatin A and PMSF protease inhibitors added fresh. Lysate proteins were separated by SDS-PAGE and transferred onto a nitrocellulose membrane. Target proteins were probed with appropriate antibodies (p14: in house antibody generously donated by Roy Duncan's Lab diluted 1:1000, Beta Actin: Sigma-Aldrich A1978 diluted 1:20000).

## Results

To investigate IFN responses to cell membrane fusion, we generated a cell line that expressed the p14 FAST protein in telomerase life-extended fibroblasts (THF) under a doxycycline inducible promoter. Expression of p14 in THF cells resulted in visible cell-cell fusion, yielding large multinucleate (syncytial) cells over time (Figure 2A). Cell membrane fusion began 8-12 hours after doxycycline treatment. Syncytial cells were not capable of dividing to produce new progeny cells, thus proceeded to die about 48 hours post induction of p14 expression. RT-qPCR of p14 transcripts was performed to confirm that doxycycline treatment did in fact induce the expression of p14 in these syncytia producing cells. Transcript levels of p14 peaked around 16 hours post doxycycline addition, diminishing somewhat over time (Figure 2B).

To assess if p14-mediated cell-cell fusion induced an IFN innate immune response, changes in the levels of interferon stimulated genes (ISGs) IFIT1 and CXCL10 were monitored over a 48-hour time course. These ISGs are common downstream products of IFN signalling in fibroblasts. Significant upregulation of IFIT1 and CXCL10 were observed 40-48 hours after doxycycline induction of p14 expression (Figure 2C). In the case of CXCL10, a temporary increase in ISG levels was observed around 16 hours post doxycycline treatment, suggesting that there may be two waves of responses, a weaker early priming response, followed by a more robust late response. Doxycycline treatment itself did not affect ISG levels in non-p14 expressing THF cells, thus the differences observed in the p14-THF cells are not influenced by doxycycline but are uniquely due to the presence of p14 in the cell and its associated fusion activity. The amount of p14 produced in cells (correlated with doxycycline concentration) did not affect the magnitude of the observed ISG response (Supplementary Figure 13). However, cell density did impact the magnitude of the ISG response, with stronger ISG upregulation occurring at higher cell density, which correlates with greater degree of cell fusion (Supplementary Figure 14). Of note, paracrine IFN signalling is more efficient at higher cell density, which also may have influenced the observed differences in ISG upregulation.

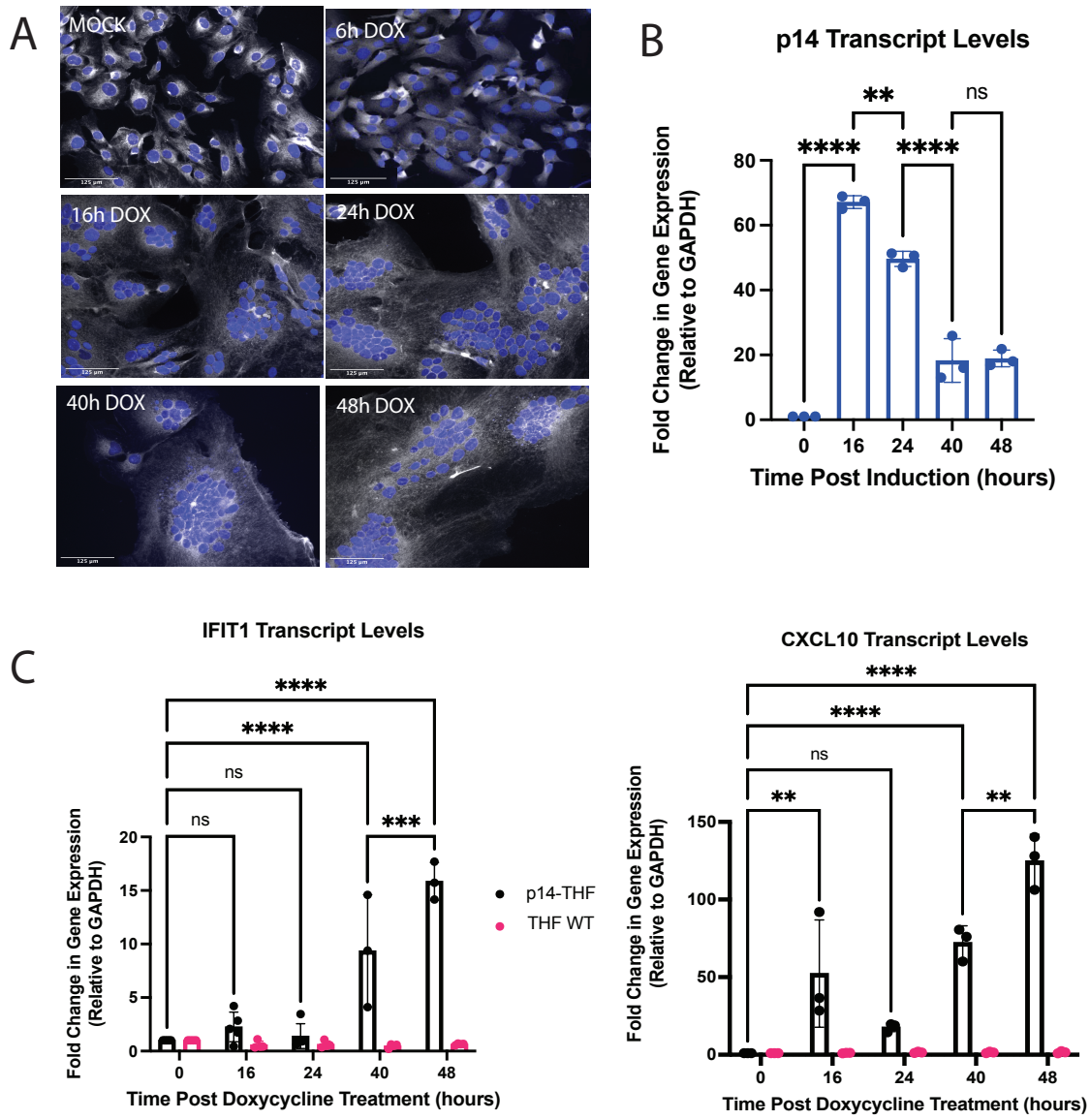


**Figure 2. Endogenous expression of p14 results in cell-cell fusion and the upregulation of interferon stimulated genes (ISGs). A)** Inducible p14-THF cells were treated with 0.01 µg/mL doxycycline and monitored over a 48 hour time period. Membrane fusion began 8-12 hours post doxycycline treatment, resulting in the formation of visible syncytia. These syncytial cells persisted for up to 48 hours before cell death occurred. Cell nuclei were stained with Hoechst 33342 and cell membranes stained with CellMask Deep Red. Scale bar indicates a size of 125 µm. **B)** Presence of p14 in the cells upon doxycycline treatment was verified by RT-qPCR. Transcript levels of p14 peaked 16 hours post doxycycline treatment, progressively dropping at later time points. **C)** To test whether p14 expression and cell fusion affects levels of ISG expression RT-qPCR was conducted over a 48 hour time course on wild type and p14-THF cells treated with 0.01 µg/mL doxycycline. Significant upregulation of IFIT1 and CXCL10 was detected 40-48 hours post doxycycline treatment in p14 expressing cells. Doxycycline had no effect on wild type THF cells.

Upregulation of ISGs can occur in the absence of IFN signalling, as some transcription factors like IRF3 can directly bind to ISG promoters and induce ISG expression independently of IFN. To test whether the upregulation of ISGs in response to cell-cell fusion is interferon dependent or independent, B18R was added in conjunction with doxycycline to serve as a decoy IFNAR receptor, effectively blocking paracrine IFN signalling. B18R treatment abolished the upregulation of ISGs normally seen in response to p14-mediated syncytia formation, suggesting that IFN is produced and ISG upregulation is a consequence of paracrine IFN signalling pathways (Figure 3A). However, the amount of IFN produced by syncytia appears to be low, since IFN could not be detected in the supernatant by VSV-GFP bioassay (Figure 3B) or in IFN-GFP reporter cells (Figure 3C).

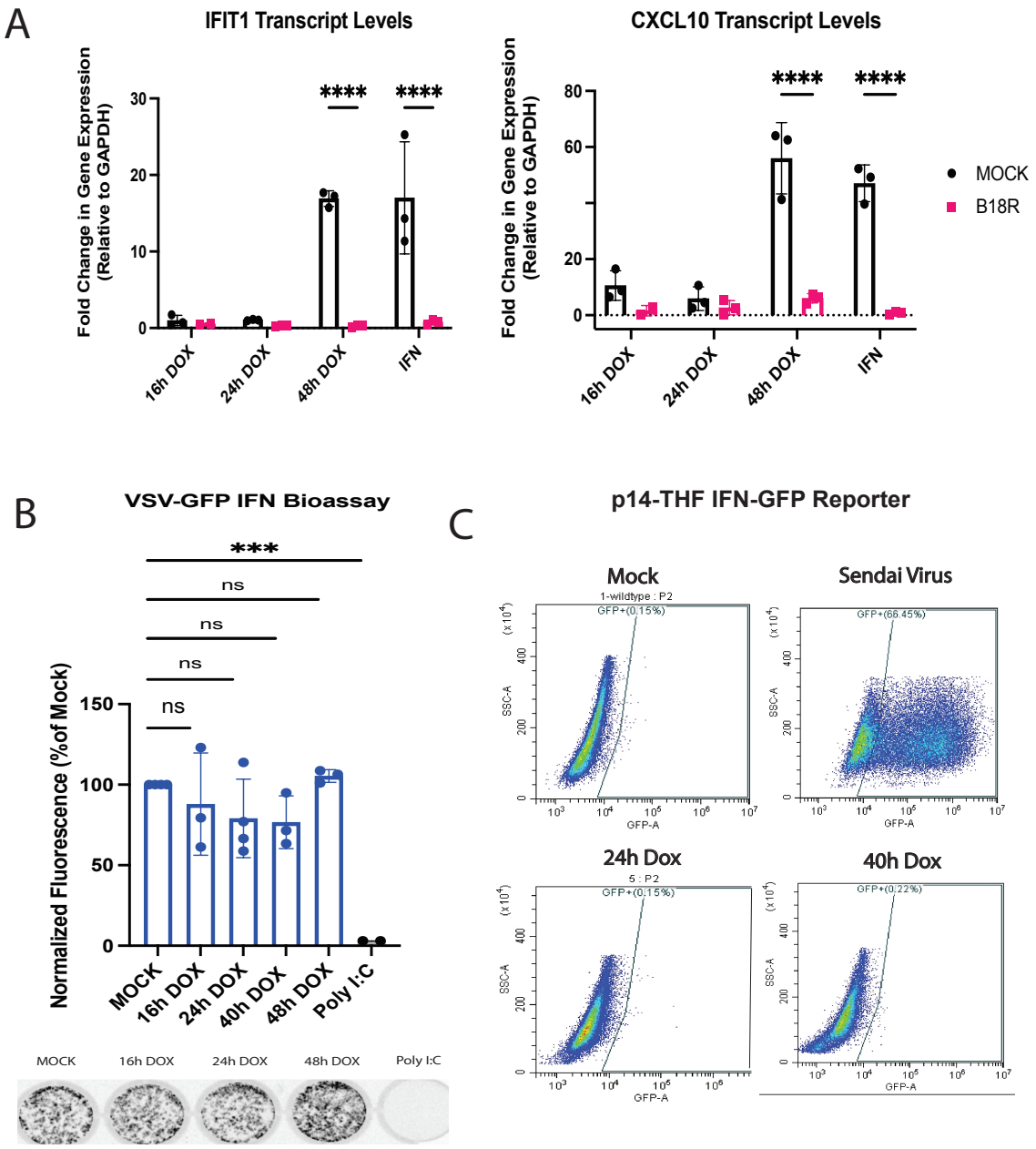


**Figure 3. p14-mediated cell-cell fusion results in the production of low level IFN**. **A)** p14-THF cells were treated with 0.01 µg/mL doxycycline for 16, 24 or 48 hours or 1000 U of IFN for 24 hours. IFN signalling was blocked with the addition of 500 ng of B18R concurrently with the doxycycline or IFN treatements. B18R blocked the upregulation of ISGs normally seen in response to p14-mediated cell fusion. **B)** Supernatants from p14-THF cells treated with 0.01 µg/mL doxycycline over time or 20 µg/mL Poly I:C were transfered onto THF-IRF3 -/- cells and incubated for 8 hours, then challenged with VSV-GFP. No significant reduction in plaques was observed **C)** p14-THF cells were modified with an IFN-GFP reporter, and the IFN-GFP positive population was isolated by flow sorting. p14-THF IFN GFP cells were then analyzed by flow cytometry to examine IFN production in response to syncytia formation. No IFN producing cells were detected upon induction of p14 expression and syncytia formation.

Conventionally, the upstream initiation of IFN signalling requires activation of key transcription factors like interferon regulatory factor 3 (IRF3). To determine if this key transcription factor is involved upstream of IFN production, IRF3 deficient THF cells were modified to express p14 under a doxycycline inducible promoter. These cells formed syncytia much like the wild type p14-THF cells, but ISG upregulation was not observed, indicating that IRF3 is required upstream of the ISG response to p14-mediated cell-cell fusion (Figure 4).

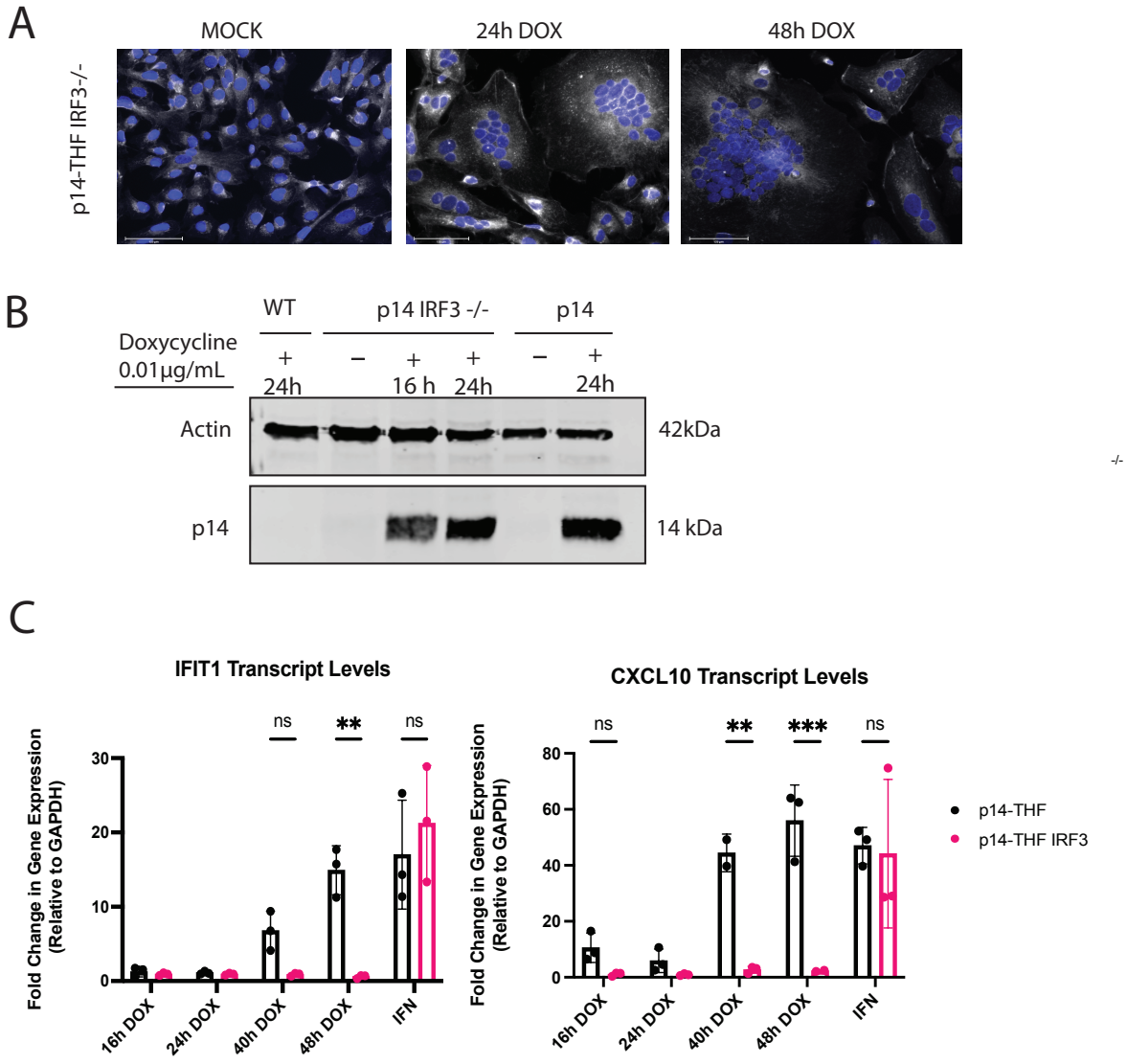


**Figure . The IFN response to p14-mediated cell-cell fusion is IRF3 dependent. A)** Cells deficient in IRF3 were modified to express p14 under a doxycycline inducible promoter. These cells are referred to as p14-THF IRF3 -/- . Much like the wild type p14-THF cells, the p14-THF IRF3 -/- cells displayed an analogous pattern of syncytia formation over time. Cell nuclei were stained with Hoechst 33342 and cell membranes stained with CellMask Deep Red. Scale bar indicates a size of 125 µm. **B)** Presence of p14 in the IRF3 knock-out cells was confirmed by western blot. Both wild type p14 and IRF3 knock-out p14 cells express similar levels of p14 upon doxycycline treatment. **C)** The p14-THF IRF3 -/- cells did not respond to the fusion process to induce expression of the ISGs IFIT1 and CXCL10, as assessed by RT-qPCR.

Various adaptors and signalling molecules can communicate signals to activate IRF3. In the case of exogenous treatment with p14 lipoplexes, RLRs were the required PRRs upstream of IRF3[92]. While we intended to test the role of RLRs in the endogenous p14 expression system, attempts to generate p14-THF RIG-I/MDA5 $^{-/-}$ cells proved challenging, as the resultant cells did not form syncytia upon p14 induction (Supplementary Figure 15). This made it difficult to discern whether the RLR deficiency or lack of cell fusion blocked the antiviral response.

Another PRR associated with membrane perturbation stress responses is STING. The predominant role of STING lies in acting as an adaptor in communicating recognition of foreign cytoplasmic DNA to IFN production. However, STING has been shown to play a role in triggering stress-based IFN responses, such as virus-like particle entry and ER stress, making it a probable signalling molecule upstream of IRF3 in the IFN response to p14-mediated cell-cell fusion. To test if STING is involved in the IFN response to p14-mediated cell-cell fusion, p14 was expressed in cells deficient in STING under a doxycycline inducible promoter. p14 expression caused extensive syncytia formation; however, no upregulation of ISGs was observed in STING deficient cells, indicating that STING is required upstream of the IFN response to p14-mediated syncytia formation (Figure 5).

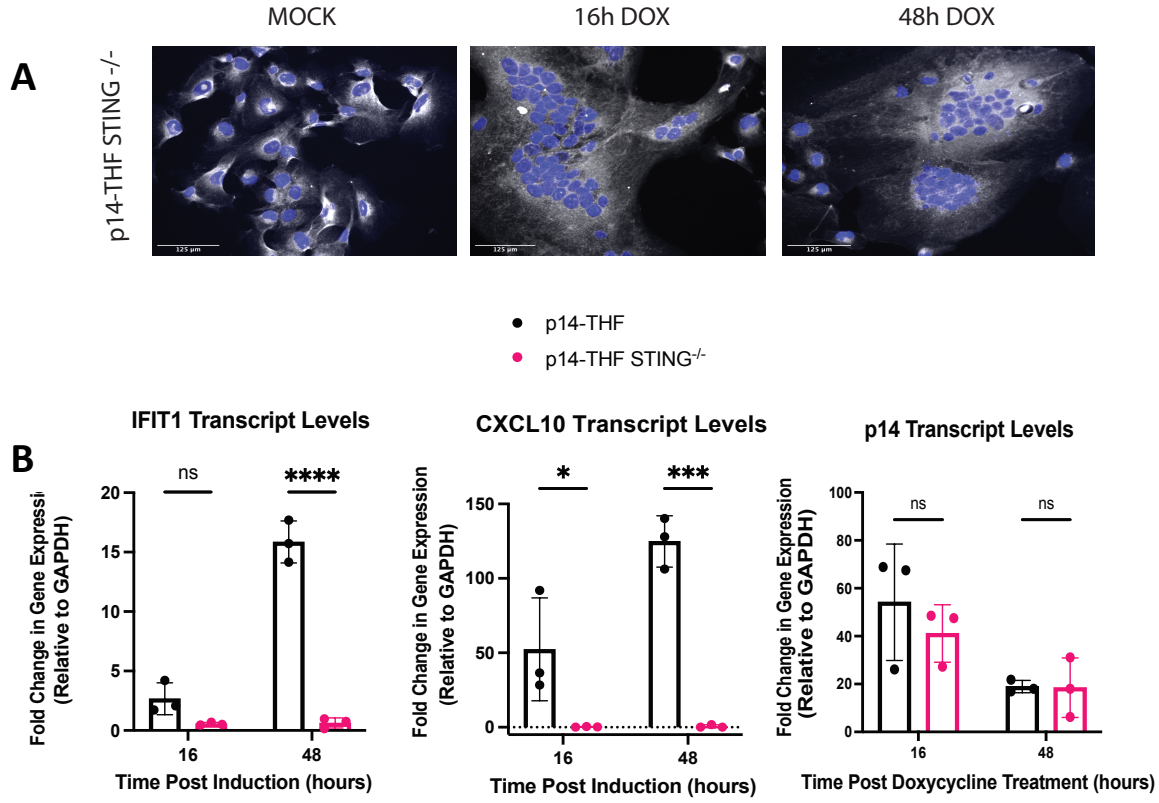


**Figure 5. The IFN response to p14-mediated cell-cell fusion requires STING. A)** Cells deficient in STING were modified to express p14 under a doxycycline inducible promoter. These cells are referred to as p14-THF STING -/- . Much like the wild type p14-THF cells, the p14-THF STING -/- cells displayed an analogous pattern of syncytia formation over time. Cell nuclei were stained with Hoechst 33342 and cell membranes stained with CellMask Deep Red. Scale bar indicates a size of 125 µm. **B)** The p14-THF STING -/- cells did not respond to the fusion process to induce expression of the ISGs IFIT1 and CXCL10, despite similar levels of p14 being expressed in both cell types.

Since the predominant role of STING entails effecting IFN signalling downstream of DNA sensing in the cytoplasm, a potential source of STING activation in syncytial cells may entail sensing of mis-compartmentalized endogenous DNA. Genotoxic stress can cause fragmentation of the nucleus, resulting in the production of micronuclei. The nuclear envelopes of micronuclei can rupture, releasing free nucleic acid into the cytoplasm, which can then be sensed by DNA sensors and activate STING. p14 syncytial cells were examined for the presence of micronuclei by fluorescence microscopy (Figure 6). Small fragments of nucleic acid resembling micronuclei were observed. Some of these micronuclei lacked nuclear lamin B1, a key structural protein of the nuclear envelope, and stained for γ-H2AX, a marker of double stranded breaks in the genome. While some DNA damage was visible 16-24 hours post doxycycline treatment, the extent of the damaged progressively worsened over time, with nearly all syncytial nuclei staining for γ-H2AX 48 hours post doxycycline treatment. This data suggests that syncytia formation driven by p14-mediated fusion results nuclear DNA fragmentation and accumulation of cytoplasmic DNA which may activate STING and subsequent IFN signalling.

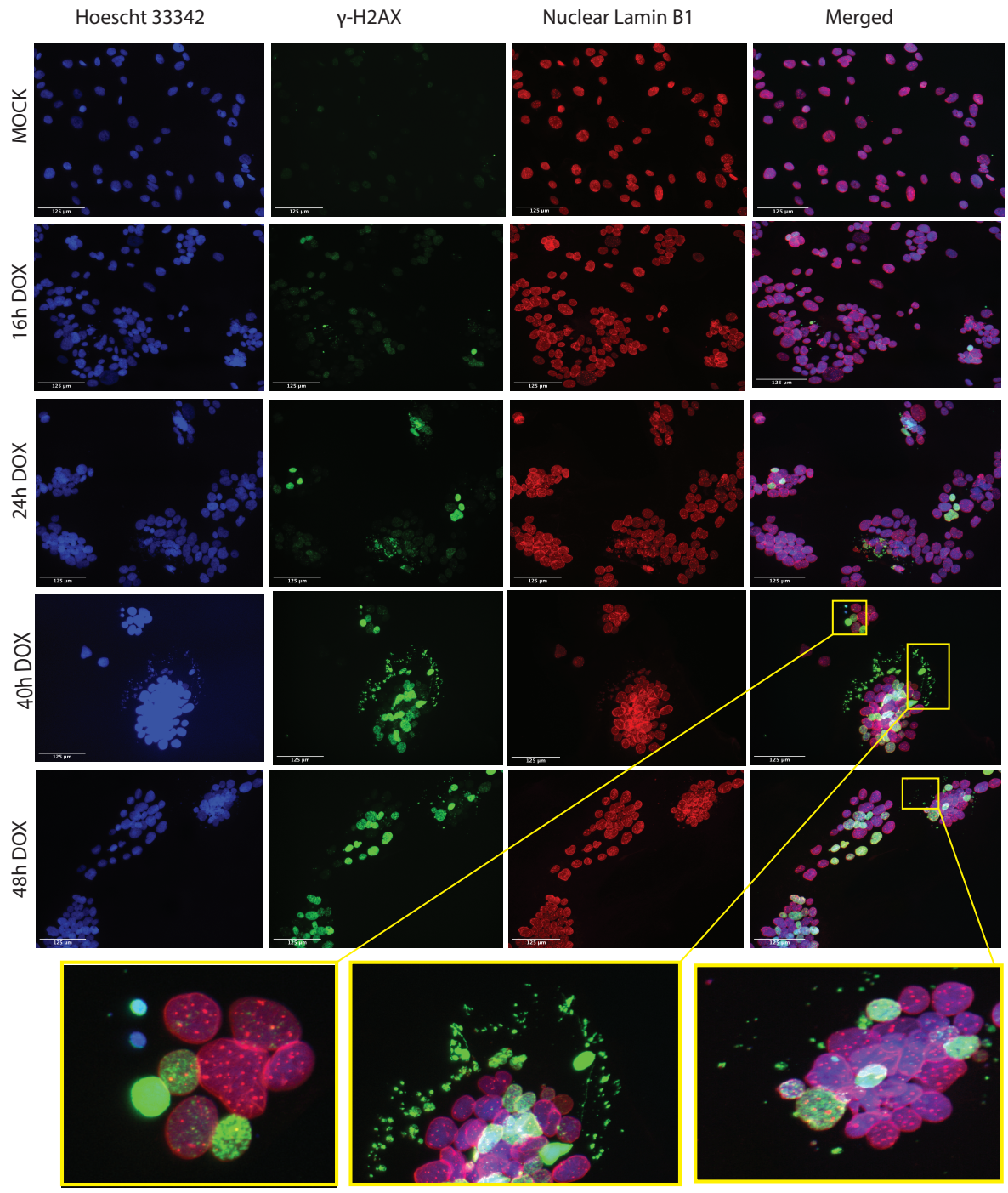


**Figure 5. Syncytial cells display markers of DNA damage and micronuclei formation**. Cell nuclei were stained with Hoechst 33342, γ-H2AX was used as a marker of double stranded breaks in the genome, and nucelar lamin B1 was used to stain for the nuclear membrane. Increasing incidence of double stranded breaks and loss of nuclear envelope integrity was observed over time. Additionally, smaller fragments of nucleic acid content resembling micronuclei are visible. These micronuclei are also often lacking in a nuclear envelope. Scale bar indicates a size of 125 µm.

While the B18R data suggests the requirement of IFN signaling in the response to p14 mediated cell fusion (Figure 3A), subsequent IFN assays suggest any IFN produced is below the limit of detection and insufficient on its own to provide full antiviral protection (Figure 3B/C). However, replication of VSV-GFP in syncytial cells was restricted if p14 expression was initiated 6 hours prior to infection (Figure 7). At the time of infection cells were still mononuclear but became multinucleated over the course of the infection. Clear syncytia are visible 12-16 hours after inducing p14 expression. In contrast, if p14 expression was initiated immediately following VSV-GFP infection, VSV-GFP replication was enhanced (Figure 7). This suggests that the kinetics of cell-cell fusion in relation to the replication cycle of a virus can influence whether syncytia formation promotes or restricts viral spread. Multiple factors may account for the observed reduction in viral plaques including: the antiviral activity of induced ISGs and low level IFN, the inability of viruses to enter syncytial cells, inhibition of protein translation, and the initiation of autophagic, apoptotic or senescence pathways. Further experiments are required as we cannot make these distinctions with the given plaque reduction assay.

Additionally, a similar plaque restricting effect was observed during HSV-GFP and VacV-GFP infections (Figure 7), suggesting that cell-cell fusion can affect the replication of various viruses, including IFN-resistant viruses like HSV, and viruses with different genomes (e.g. DNA vs RNA) and modes of replication (e.g. nuclear vs cytoplasmic). Unlike VSV-GFP, HSV-GFP and VacV-GFP replication was not enhanced by late cell fusion (Figure 7), suggesting that while syncytia formation can be beneficial to VSV replication, it may not be an advantageous feature for HSV and VacV.

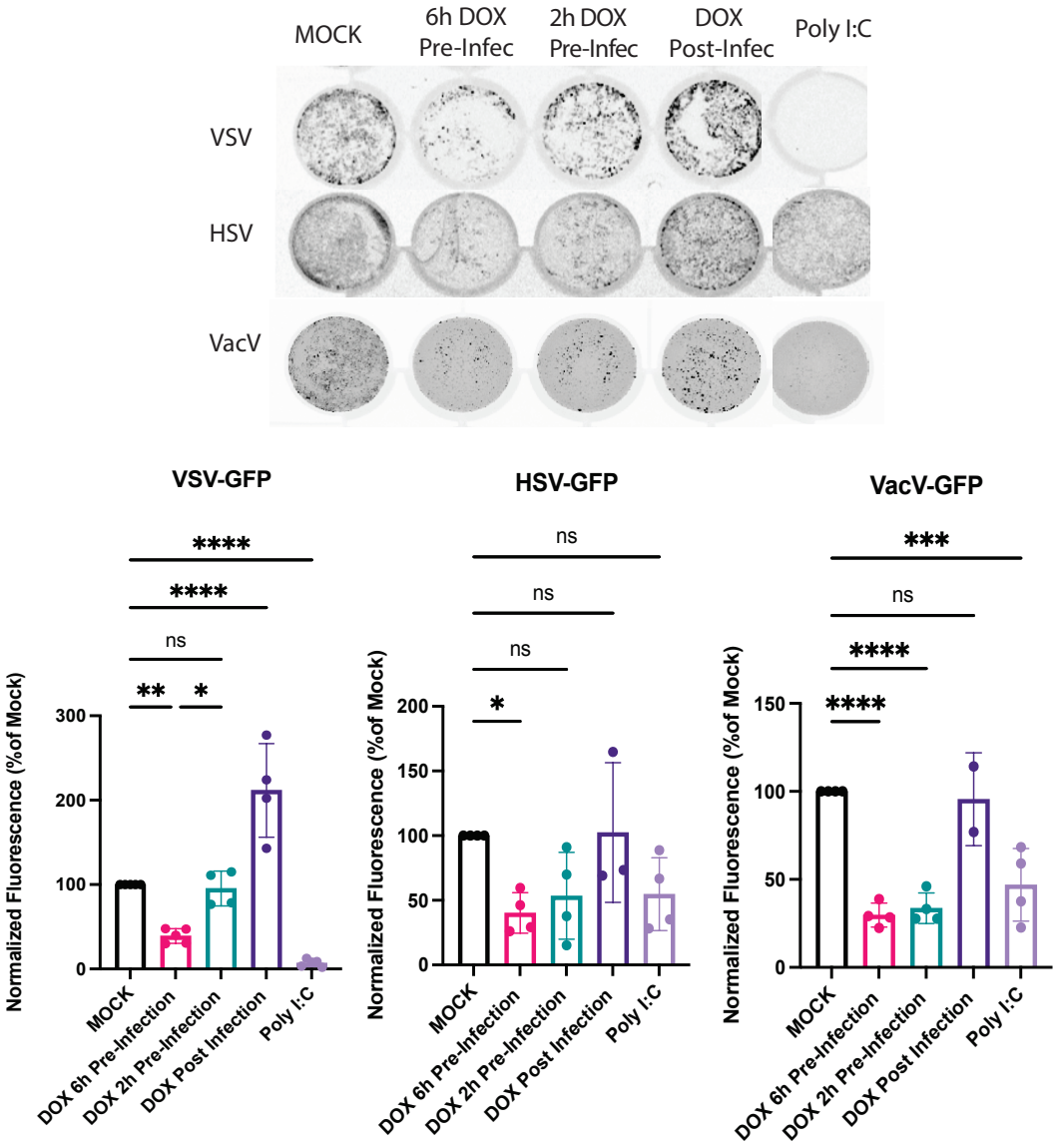


**Figure . Syncytia formation can enhance or impair viral replication depending on when syncytia formation occurs relative to the replication cycle of the virus.** The effect of p14-mediated cell fusion on viral replication was assessed by infecting cells with VSV-GFP, HSV-GFP, and VacV-GFP and monitoring plaque formation by GFP fluorescence. p14-THF cells were treated with 0.01 µg/mL doxycycline 6 hours prior to infection, 2 hours prior to infection or immediately following virus infection. Plates were scanned 20 hours post infection on a Typhoon scanner and fluorescence intensity was quantified using ImageQuant software. When p14 is present in the cells and cell fusion occurs early on during the infection, there is a significant reduction in plaques; however, when p14 is expressed later in the replication cycle of the virus viral replication is enhanced.

While at first glance it seemed that early p14 expression and cell fusion during an infection could induce an antiviral state, the observed reduction in plaques was found to occur in the absence of IRF3 and when IFN was blocked by B18R, suggesting that IFN signalling is not involved in restricting viral replication in syncytial cells (Figure 8). However, no plaque reduction was observed in STING deficient cells, suggesting that STING is involved in the cellular pathway or mechanism initiated by cell fusion that restricts viral replication or spread (Figure 8). The enhanced viral replication that occurs in the case of late fusion during an infection was not affected neither by the removal of IRF3, STING nor IFN blockade.

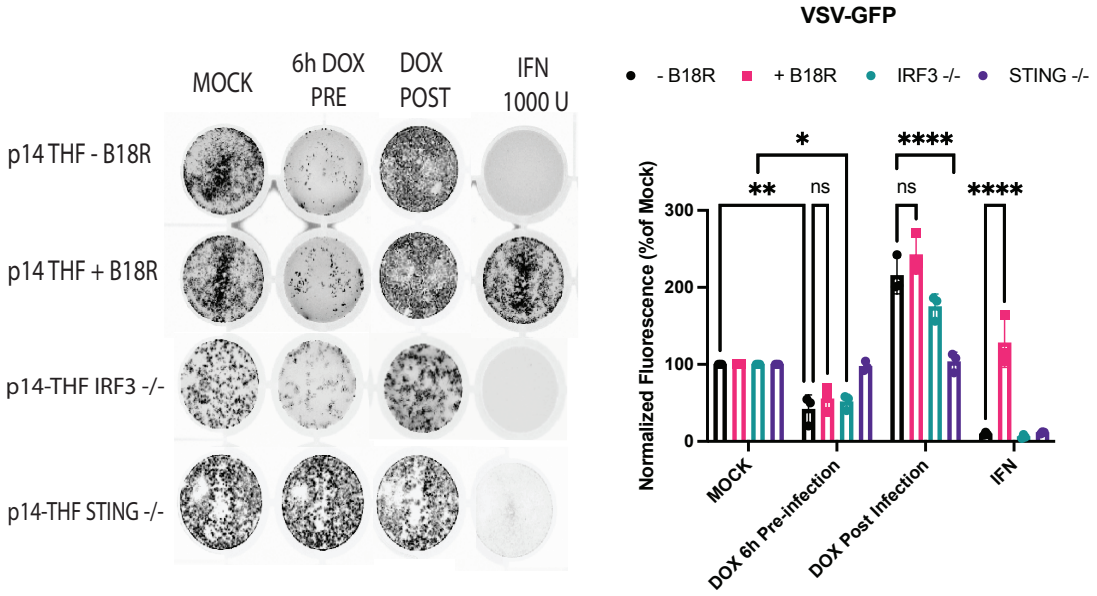


**Figure 7. Differences in viral replication in syncytial cells are IFN and IRF3 independent, and STING dependent**. VSV-GFP plaque reduction assay was conducted to assess if p14-mediated cell fusion induces an antiviral response that can restrict VSV replication. p14-THF cells, p14-THF IRF3 -/- cells and p14-THF STING -/- cells were treated with 0.01 µg/mL doxycycline 6 hours prior to infection or immediately following infection with VSV-GFP. 500 ng of B18R was added at the same time as doxycycline to block any IFN signalling. Plates were scanned 20 hours post infection on a Typhoon scanner and fluorescence intensity was quantified using ImageQuant software. The reduction in plaques observed after 6h of doxyxycline pre-treatment was not affected by B18R IFN inhibition, nor by the elimination of IRF3. However, elimination of STING abolished this effect.

## Discussion

We initially hypothesized that endogenous expression of p14 and cell-cell fusion would induce membrane perturbation associated IFN responses analogous to those observed following p14 lipoplex entry. Thus, we expected to see an IRF3 and RLR dependent antiviral response, with low level IFN production[90–92]. Our investigation with the endogenous p14 fusion system illustrates that endogenous p14 expression and fusion, like exogenous p14, can stimulate the upregulation of ISGs in an IRF3 dependent manner and low level IFN is required for this response. However, the mechanism that leads to an ISG response appears to be different across the two systems, as the response to p14 lipoplex treatment involves RLRs and MAVS, while the response to endogenous p14 requires STING[92]. Although in one case RNA sensors are required and in the other DNA sensors are required, nucleic acid sensing is a key common feature of both types of p14 responses. Differences in p14 activity may account for the involvement of different signalling pathways. Endogenous p14 expression results in the accumulation of p14 at the cell membrane and cell-cell fusion. In the case of exogenous p14 lipoplexes, the fusion domain of p14 is required for an antiviral response, but it is not clear whether p14 lipoplexes fuse at the cell membrane or enter by endocytosis and fuse at internal membranes, which may impact downstream signalling[90]. The multinucleated state of cells following endogenous p14 expression could also alter cellular processes.

Typically, the induction of ISGs is indicative of IFN production and an antiviral state. Our data shows that p14 expression and cell-cell fusion induces ISG upregulation, and this response requires STING, IRF3, and low level IFN. Contrarily, early p14 expression and cell fusion induces an antiviral state independently of IRF3 and IFN, though STING is still required, creating a discrepancy between the observed ISG induction and antiviral state. The ISGs we chose to monitor are some of the most highly and most consistently upregulated, and associated with antiviral responses in fibroblasts, but there is limited knowledge of which ISGs are essential for specific cellular responses and at what levels. Thus, while IFIT1 and CXCL10 may be upregulated in response to p14 cell fusion, these ISGs may or may not play a role in the host response to p14, while other ISGs that were not monitored may contribute to the antiviral state. Based on our current data, it appears that p14 syncytial cells can restrict viral spread by an IFN and IRF3 independent, but STING dependent antiviral mechanism. This mechanism may entail an NF-κB pathway, a novel form of antiviral response or be a consequence of other pathways occurring in the stressed syncytial cells that compromise virus entry and/or replication processes. The adaptor STING has been implicated in a multitude of cellular pathways other than IFN signalling, some of which include the pro-inflammatory NF-κB pathway, modulation of senescence, protein translation, autophagy, and other modes of cell death[96,97]. Several studies highlight a role for STING in initiating the ancient antiviral mechanism of autophagy, particularly in response to ER stress induced UPR[98]. A recent study described the TBK1-dependent and IRF3-independent manner in which STING signalling induced autophagy, promoting resistance to HSV-1 in vivo[99]. Regulating the balance between autophagy and protein

translation initiation in a cell is one of many roles of the PI3K/mTORC1 pathway. In p14 syncytial cells p70-S6 kinase, a downstream product of mTORC1 signalling was activated (Supplementary, Figure 16), which is a marker of active protein translation initiation and autophagy inhibition. While this piece of data is preliminary and provides an incomplete analysis of mTOR signals associated with cell fusion, it hints that mTOR mediated autophagy is an unlikely contributor to the antiviral response of p14 syncytial cell, although STING-associated activation of autophagy may still be involved by alternative mechanisms. Recent findings also suggest that the cGAS-STING pathway can activate the senescence-associated secretory phenotype (SASP) in response to the accumulation of cytoplasmic DNA[100]. SASP describes the phenomenon whereby senescent cells secrete inflammatory cytokines, chemokines growth factors and matrix metalloproteinases[100]. Considering that syncytial cells do not divide, it is likely that they enter a senescent state. Studies have shown that viral replication is significantly impaired in senescent cells and cells that have sustained nuclear damage[14,15,101]. Thus, senescence and the SASP may explain the restricted viral replication in syncytial cells, although more work needs to be done to confirm this theory and fully understand the mechanism of the response.

Furthermore, our investigation of cell fusion responses showed that p14 FAST fusion protein mediated cell-cell fusion results in dsDNA breaks and the accumulation of DNA in the cytoplasm, which can induce a type I IFN response through STING-IRF3 signalling. These findings are consistent with prior work claiming that MeV-induced cell-cell fusion amplified IFN responses in infected cells through IRF3[102]. Two more recent reports show that bacterial induced cell-cell fusion triggers the cGAS-STING pathway via micronuclei formation, and sensing of cytoplasmic chromatin by cGAS activates innate immune responses in SARS-CoV-2 induced syncytia [42,103]. The analogous findings across all these different cell-cell fusion systems suggests that DNA-damage induced IFN responses may be a common feature of all syncytial cells, regardless of the type of fusogen involved.

Previous work that investigated IFN responses to membrane perturbations using virus particles proposed that membrane perturbations caused by enveloped virus entry can be sensed by the cell as a form of stress, and signal the cell to initiate innate immune responses in preparation for counteracting an infection[1,3,18,86,88]. While this may be the case for virus envelope-cell membrane fusion and warrants further investigation, the delayed ISG upregulation we observed in syncytial cells (28-32 hours after cell fusion) does not seem to be a direct effect of the fusion process itself, but rather a consequence of biological changes in the cell resulting from existing in a multinucleated state. Multinucleation puts stress on the cell division machinery, as the cell is not equipped to mediate simultaneous division of multiple nuclei. Syncytial cells have been shown to undergo abortive mitosis, where the genetic content attempted to reshuffle, but mitotic chromosomes were not pulled to opposite poles of the cell, and points of constriction were visible at the cell membrane, but they dissipated instead of producing daughter cells[104]. Our data also showed progressively worsening DNA damage and cytosolic DNA accumulation in p14 syncytial cells over time, which is a known trigger of cGAS-

STING-IFN responses[105]. Thus, micronuclei formation and release of DNA into the cytoplasm appears to be a consequence of syncytia formation and can serve as a possible trigger of the observed ISG responses. The mechanistic details of how DNA damage occurs in syncytial cells remain elusive and is an interesting question for future research.

While prototypic IFN assays (IFN-GFP promoter assay) and IFN activity assays (supernatant transfers) failed to detect IFN, data with B18R suggests that low level IFN signalling is critical to the observed ISG response to p14 induced cell fusion. The low level IFN response in p14 syncytial cells is much weaker than typically seen with canonical PRR activators like the mimetic of foreign nucleic acid Poly I:C. The extensive cellular DNA damage repair mechanisms and methods for distinguishing self from foreign nucleic acids may be responsible for this discrepancy[106,107]. Also, self-nucleic acids are degraded much more rapidly in the cytoplasm than foreign nucleic, decreasing their chances of detection by PRRs, and cells can activate autophagy to cope with DNA damage and the accumulation of micronuclei[107]. Thus, deficiencies in the DDR pathways could allow for stronger syncytial IFN responses. Cancer cells in particular harbour defects in elements of DDR pathway[106,108]. In fact, mutations or chromosomal aberrations that result from faulty DNA repair are considered causal factors for cancer development, as they can activate oncogenes or inactivate tumor suppressor genes and initiate the malignant transformation of previously healthy cells into cancerous cells[106]. Interestingly, while DNA damage can drive oncogenesis, it also plays a dual role in tumor suppression. Persistent double stranded breaks caused by endogenous and exogenous genotoxic agents such as ROS, UV or ionizing radiation, and chemotherapeutic or industrial chemicals result in cellular senescence, apoptosis and tumor suppression, and are therefore commonly incorporated into cancer treatment strategies. Recent work has also highlighted the role of DNA damage in innate immunity and proposed it as a novel target for cancer immunotherapy[108]. Syncytial oncolytic viruses may be an excellent strategy for inducing tumor-specific DNA damage with immunotherapeutic benefits.

Syncytial viruses have been proposed as a potential solution to overcoming the challenge of limited viral spread in oncolytic virotherapy treatments and have recently been gaining popularity with mixed results[109]. The syncytial phenotype should allow rapid viral spread and enhance bystander cell killing, while maintaining oncotropic specificity[109]. However, it is important to keep in mind that there is a fine balance between cell death and viral replication, and excessive cell-cell fusion could hinder viral replication and spread if the cells experience too much cytotoxicity. Another advantage of syncytial oncolytic virotherapy is its ability to increase immune cell infiltration to the tumor[109]. Why syncytial oncolytic viruses are more effective at increasing tumor immunogenicity is not yet clear, but the secretion of inflammatory cytokines like IFN in response to syncytia formation and associated DNA damage may be an important contributing factor. FAST proteins are particularly attractive candidates for engineering syncytial oncolytic viruses as they are the smallest viral fusion proteins, which allows for easy insertion into the viral genome. Several groups are testing p14-modified syncytial oncolytic viruses as potential candidates for cancer therapy[110,111]. Preliminary results indicate these viruses have

enhanced efficacy at reducing tumours in some cell types but not others. Understanding the biology of syncytial cells and how they initiate innate immune responses may aid the development of more targeted and effective oncolytic viral therapies in the future.

In the context of a naturally occurring syncytial virus infection, it is unlikely that the low level syncytial IFN response alone is sufficient to provide host protection against the virus. Interestingly, a study of MV showed that syncytia formation by the MV fusion proteins alone did not produce measurable IFN, but the IFN response to the fusogenic virus was enhanced compared to its non-fusogenic analog[102]. This suggests that there may be a synergistic effect between syncytial and canonical IFN responses. From an evolutionary perspective, the conservation of the syncytial phenotype in select viruses must mean that the feature provides the virus with a selective advantage over non-syncytial counterparts. We have shown that syncytia formation can enhance virus replication, but it can also impair it. The kinetics of cell fusion relative to the replication cycle of the virus is an important consideration for achieving a benefit from syncytia formation, as premature fusion can restrict viral spread. In the case of reoviruses, translation initiation from suboptimal translation start codons and extensive degradation by ER-associated degradation pathways delays accrual of FAST proteins at the cell membrane, synchronizing cell fusion to late stages of the virus replication cycle[71]. Other syncytial viruses must also have ways of ensuring proper timing of cell fusion to maximize benefit from syncytia formation.

## Concluding Remarks

A syncytial phenotype has been considered as a selective advantage for a virus as it should enhance cell-cell spread. However, only a small proportion of viruses demonstrate a syncytial phenotype and a selective advantage in vivo, raising questions as to whether syncytia formation is as advantageous as originally thought. We hypothesized that syncytia formation can trigger stress-based innate immune responses as a protective countermeasure.

Our investigation showed that syncytia formation alone can trigger low level IFN responses and the upregulation of ISGs through an intermediate event of nuclear DNA fragmentation. These results highlight a role for nucleic acid sensors in membrane perturbation associated stress responses. This stress induced IFN response adds an extra layer of innate immunity that may synergize with conventional PAMP detection based IFN responses and enhance antiviral immunity.

Additionally, we have shown that extensive genotoxicity accompanies syncytia formation, highlighting the enhanced cytopathic effects of syncytial viruses. Syncytial viruses must manage a fine balance between their replication cycles and cytotoxic effects, as premature cell senescence or death will impair further propagation of the virus. Hence, synchronizing syncytia formation with late stages of a virus infection is an important feature for maximizing the cell-cell spread benefits of syncytial viruses.

While many questions remain regarding the syncytial phenotype and its effects on both the virus and the host, this study provides some insight into cell fusion induced innate immune antiviral responses and highlights STING as a key player in the process.

# Appendix 1: The Role of Calcium in Antiviral Responses

## Background

### *Calcium as a Messenger*

The calcium ion ($Ca^{2+}$) is an extremely versatile messenger that can respond to both extrinsic and intrinsic stimuli in all cell types. The information carried by a calcium signal is encoded in the frequency, kinetics, amplitude, and spatial extent of the oscillation, and varies depending on the type and intensity of stimulation [112,113]. For instance, the frequency of oscillation is directly proportional to the intensity of the applied stimulus [112,113].The basal cytosolic calcium concentration is maintained at about 100 nM [112]. When the cytosolic calcium concentration changes due to calcium influx from the extracellular fluid or from intracellular calcium stores like the ER and mitochondria, it provokes a cellular response [114]. A sustained increase in cytosolic calcium activates apoptotic programs; whereas, transient oscillating calcium signals activate proliferation and pro-survival pathways [112,115].

Calcium oscillatory signals are largely decoded through the phosphorylation-dependent control of calcium-activated kinases and phosphatases, such as calmodulin-dependent kinase II (CaMKII) and calcineurin [112,116]. Recent evidence illustrates that phosphorylated and calcium loaded calmodulin binds PI3Kα at its SH2 domains, initiating the PI3Kα/Akt signalling pathway, which promotes cell proliferation [117]. The PI3K/Akt pathway has been implicated in the host cell immune response through regulation of the transcriptional repressor EMSY to induce the transcription of a subset of ISGs [118]. PI3K pathways have been implicated in the antiviral response to membrane perturbation, highlighting a link between calcium signalling and membrane fusion of enveloped viruses [119,120].

Recent findings illuminate additional evidence of a role for calcium signalling in the innate immune system via the cGAS-STING axis [121]. STING activation can be regulated through the binding of calcium by its dimer [122]. Additionally, the interaction of STING with STIM1, a regulator of store-operated calcium entry, anchors the two proteins to the endoplasmic reticulum (ER), which influences their individual activity and links calcium regulation with type I interferon signalling pathways [14,15]. STING can also directly interact with numerous calcium channels, such as SERCA2, ATP2B1, VDAC1, and VDAC3, suggesting that STING when activated may regulate $Ca^{2+}$ flux within the cell through such interactions [123].

Prior work in our lab demonstrated that the antiviral response to UV-inactivated enveloped virus particles and the p14 FAST protein lipoplexes triggered cytosolic $Ca^{2+}$ oscillations [18]. Inhibition of $Ca^{2+}$ flux by 2-ABP, an inhibitor of calcium release from intracellular stores, completely blocked the antiviral response to p14 and partially blocked the response to UV-inactivated virus particles [18]. Fusogenic liposomes could induce a $Ca^{2+}$ flux but no antiviral response, suggesting that $Ca^{2+}$ is necessary but not sufficient for the antiviral

response to membrane perturbations[92]. We hypothesized that specific calcium signals at specific cellular locations are required to achieve an antiviral state following membrane perturbations.

***Genetically Encoded Calcium Indicators***

To address our hypothesis, we decided to use genetically encoded calcium indicators (GECIs) to better characterize and localize calcium signals. GECIs are calcium binding proteins that consist of two domains: a calcium-binding domain derived from calmodulin, and a fluorophore domain (Illustrated in Figure 3) [124]. The protein dynamics between the two domains are engineered such that the GECI will produce a fluorescence signal in the calcium bound but not free state [125]. A wide range of GECIs have been designed to target different intracellular compartments by introducing localization tags and modifying the binding affinity ($K_d$) of the calcium binding domain, such that it is within the dynamic range of the cellular calcium concentration ranges in the given compartment.

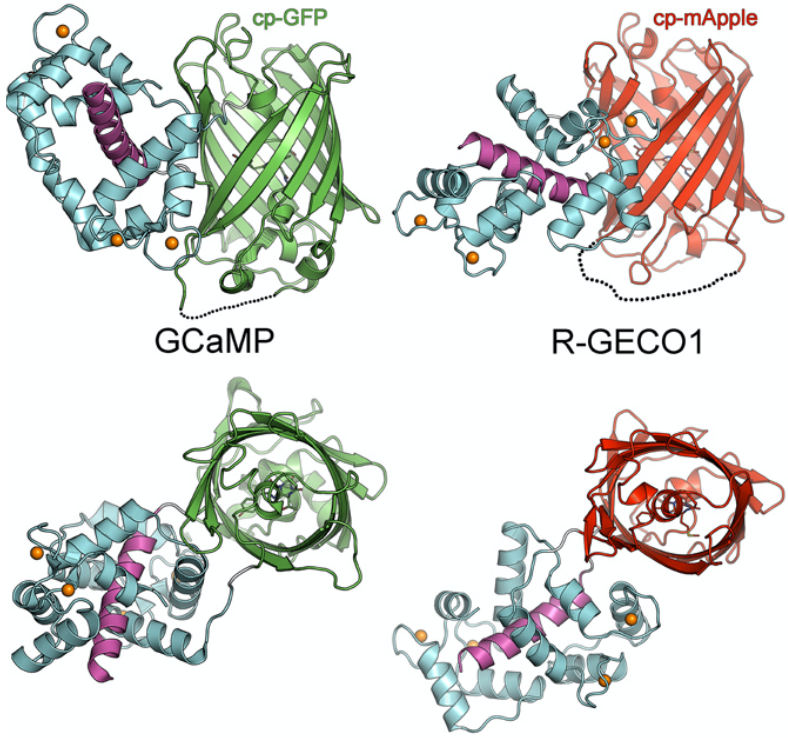


**Figure 8.** Ribbon Diagrams of two types of GECIs: GCaMP and RGECO
*Adapted from Jasper Akerboom, Front .Mol. Neurosci. 2013 March 4*

We obtained three GECIs from the Hyser Group: GCaMP6s (cytosolic), GCAMP6s-CAAX (cell membrane anchored), and RGECO1 (ER localized). These GECIs should help us visualize calcium fluxes and localize the sources of calcium release upon enveloped virus particle entry. If the cytosolic calcium oscillations are due to extracellular calcium influx, the GCAMP6s-CAAX will respond. If the calcium oscillations originate from an intracellular calcium store the ER, which is the largest store of intracellular calcium, is the most probable

source, and the RGECO1 GECI will respond most actively. Following identification of calcium localization, key receptors, kinases, and signalling proteins involved in this antiviral calcium signalling pathway can be identified by assessing the effects of targeted inhibitors. Knock-down experiments can further confirm essential protein players, as inhibitors come with a caveat of being prone to generate off-target effects.

## Materials and Methods

### *Generation of Cell Lines*

All cell lines were generated using the same PiggyBac system used to make the inducible p14-THF system described previously.

### *Live Cell Microscopy*

GECI transduced THF cells were seeded onto a Nunc Lab-Tek 2-well Chambered Coverglass (ThermoFisher Scientific) and GECI expression induced with 0.01μg/mL doxycycline. 30 minutes prior to imaging, the media was replaced with FluoroBrite DMEM (ThermoFisher Scientific) containing 1% L-Glu and 25mM HEPES, or UV-inactivated HSV (MOI of 10) in the same media. Time course imaging was acquired on an Evos FL Auto 2 Widefield Microscope for a period of 1 hour, with shifting between mock and treated samples at 2 locations. The sample remained incubated at 37°C and 5% $CO_2$ throughout the imaging process. Fluorescence intensity changes were quantified using ImageJ software, and compared in terms of normalized corrected total cell fluorescence (CTCF), where CTCF=Integrated Density – (Area of selected cell X Mean fluorescence of background readings).

### *Virus Particle UV-Inactivation*

HSV was diluted in FluoroBrite DMEM containing 1% L-Glu and 25mM HEPES to an MOI of 10 as per the following calculation:

$$\frac{Multiplicity\ of\ infection\ (\frac{pfu}{cell})}{HSV\ titre\ (\frac{pfu}{mL})} \times Cell\ count\ \left(\frac{cells}{well}\right) \times \frac{Dilution\ volume\ (mL)}{Infection\ volume\ (\frac{mL}{well})}$$

500 μL of diluted virus was aliquoted into a 12-well plate and UV-inactivated at 6000μJ.

## Results and Discussion

### *Assessing Functionality of GECI cells*

GECI transduced THF clones were screened by treating the cells with thapsigargin, a drug that depletes ER calcium stores by stimulating calcium release and accumulation in the cytosol. Thus, we expect thapsigargin treatment to trigger a significant change in fluorescence signal in GECI expressing cells. Clones that displayed a significant change in fluorescence upon thapsigargin treatment with minimal background were selected for further studies.

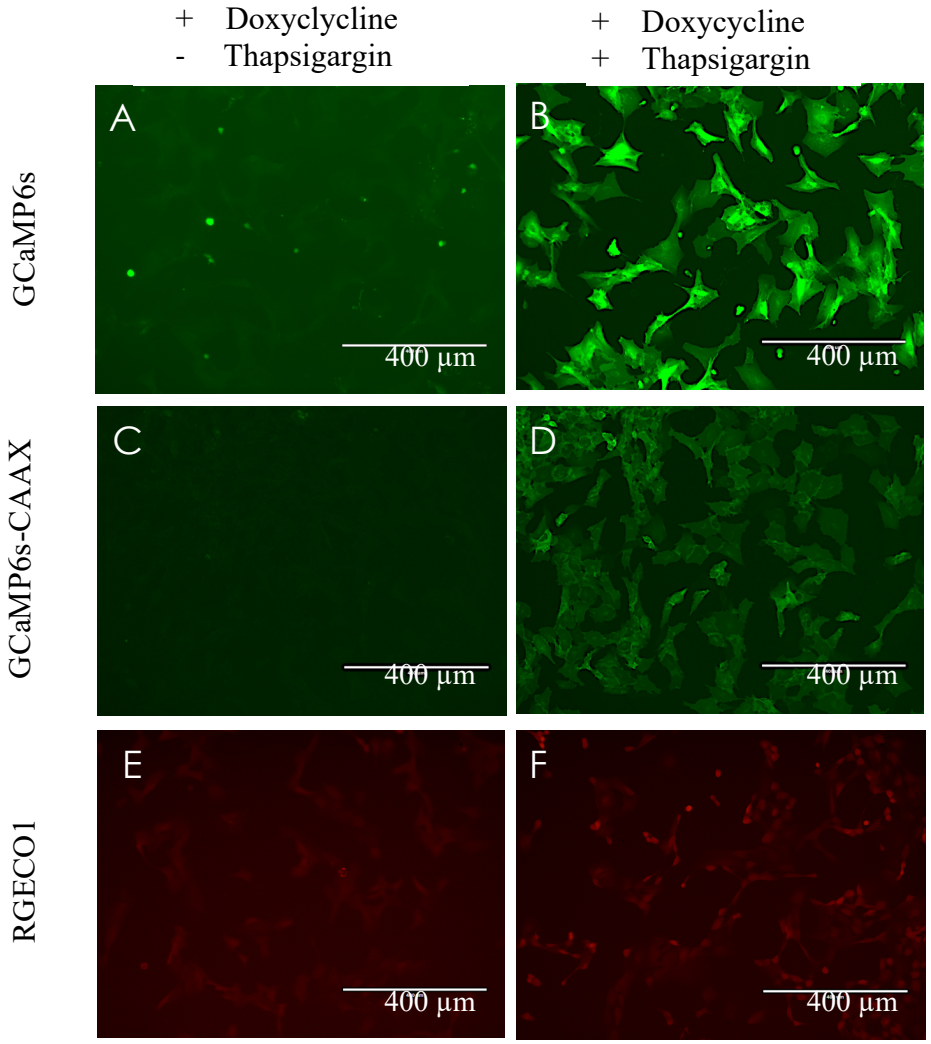


**Figure 9.** Response potential of GECI transduced THF cells, GCaMP6s (A and B), GCaMP6s-CAAX (C and D) and RGECO1 (E and F). The left panel (A, C, E) depict cells treated with doxycycline (1µg/mL) for 24 hours. The right panels (B, D, F) depict cells treated with doxycycline (1µg/mL) for 24 hours followed by treatment with the calcium releasing drug thapsigargin (1 µM). Images were taken within 30 minutes of thapsigargin treatment. Scale bar indicates a size of 400 µm.

As expected, thapsigargin treatment in doxycycline induced cells resulted in an increase in fluorescence intensity of the GCaMP6s and GCaMP6s-CAAX GECIs, as cytosolic calcium concentration increased. The fluorescence signal was also more concentrated near the cell membrane in the GCaMP6s-CAAX GECI, confirming cell membrane anchoring of this GECI. RGECO1 also responded to the thapsigargin treatment with a small fluorescence increase, suggesting that RGECO1 may localize on the cytosolic side of the ER rather than inside the ER. However, from these images (Figure 10) it is difficult to confirm whether RGECO1 is in fact ER localized at all, and further characterization of this GECI should be done to confirm its functionality. Additionally, the RGECO1 cells morphologically appeared somewhat stressed, which could have also influenced our observations.

***Kinetic Fluorescence Microscopy***

Live cell, kinetic fluorescence microscopy experiments were performed to test if calcium oscillations can be seen in the various GECI-transduced THF cells following HSV-UV treatment. Flickering of cells was observed in GCaMP6s-CAAX THF cells treated with HSV-UV, and when these fluorescence changes were quantified and compared to that of mock treated cells, an oscillatory pattern in the fluorescence intensity was confirmed (Figure 11). Neither cell flickering, nor oscillations in fluorescence intensity were seen in GCaMP6s THF cells (Figure 11). Since GCaMP6s-CAAX localizes to the cell membrane, this data suggests that HSV-UV entry into cells triggers calcium flux across the cell membrane, and signalling proteins at the cell membrane with known calcium-associated functions may be involved in communicating the calcium flux to pattern recognition receptors. While virus particle entry appears to trigger cell membrane localized calcium oscillations, we cannot yet conclude whether this calcium flux is associated with the antiviral response to membrane perturbation. Additional delayed calcium signals and signals from other calcium stores may also be involved. Longer time frame live cell imaging would be informative in understanding all related calcium signals; however, cells visibly began to stress about an hour into imaging despite the incubated stage and minimized light exposure, posing a challenge for such experiments. Analogous experiments with the ER-localized GECI (RGECO1) still need to be conducted to see if ER calcium is involved in fusion triggered calcium oscillations. Initial trials with the RGECO1 GECI faced the challenge of weak fluorescence signal, which made it difficult to detect any changes.

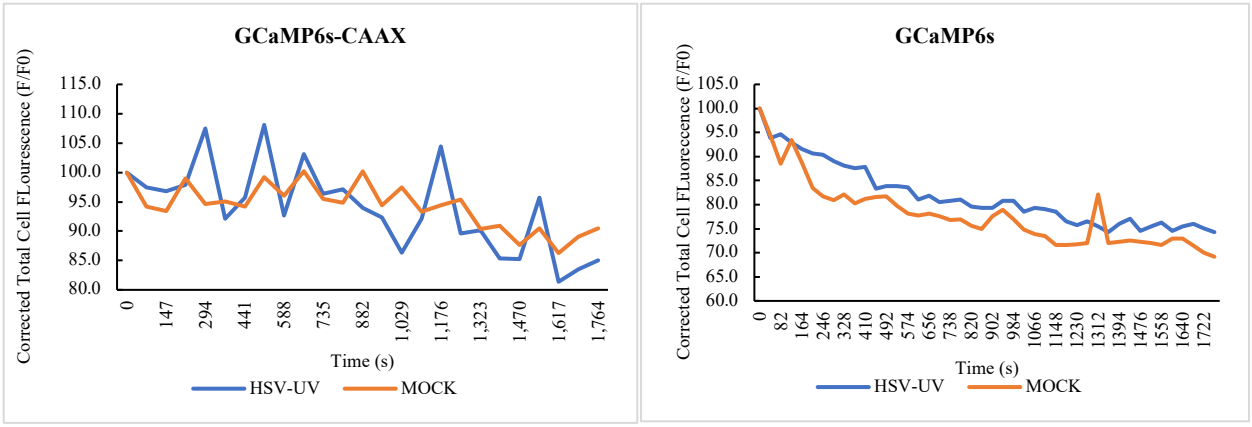


**Figure 10.** Calcium oscillations were observed in GCaMP6s-CAAX cells 30 minutes post treatment with HSV-UV virus particles, but not in analogously treated GCaMP6s cells. The period of each oscillation was about 2 minutes long, and the oscillations persisted for about half an hour.

### *Calcium Inhibition: Endogenous p14 fusion and ISG response*

We have previously seen that treating cells with p14 lipoplexes triggers calcium oscillations in the cell. Blocking these calcium fluctuations with inhibitors, such as BAPTA-AM (a calcium chelator), and 2-APB (an inhibitor of the inositol triphosphate channel) resulted in a loss of antiviral response to p14 lipoplexes. To test whether calcium signalling is also important in the innate immune response to p14-mediated cell-cell fusion, p14-THF cells were treated with these calcium inhibitory drugs in the presence of doxycycline. Changes in the fusion capacity of p14 upon calcium inhibition were visually monitored by examining the extent of syncytia formation (Fig. 12A), and the antiviral response upon drug treatment was monitored by RT-qPCR of ISGs (Fig. 12B). 2-APB prevented syncytia formation at the higher concentration of 200 µM, but not at the lower concentration of 50 µM. The effect of 2-APB on the antiviral response to p14 corresponded to its effect on fusion, whereby the higher concentration of the drug blocked the antiviral response, while the lower concentration did not. BAPTA-AM did not affect p14 fusion capacity, although it did slow down the process. Of note, BAPTA-AM may wear off over the long time frame of treatment, as replenishing cells with fresh BAPTA-AM every 12 hours resulted in significant toxicity.

Regardless of effective syncytia formation, both 200 µM 2-APB and BAPTA blocked the antiviral response to p14. While this suggests that calcium is important for both p14-mediated fusion, and the downstream antiviral signalling cascades, it is difficult to understand and differentiate these calcium signals with inhibitors alone since calcium signalling is involved in a plethora of different cellular processes. Future work should focus on optimizing long term calcium imaging experiments with the GECIs or alternate calcium indicators and combine this technique with inhibitory drugs to help us better understand the complex calcium signals involved in membrane perturbations by virus-cell and cell-cell fusion and the associated antiviral responses.

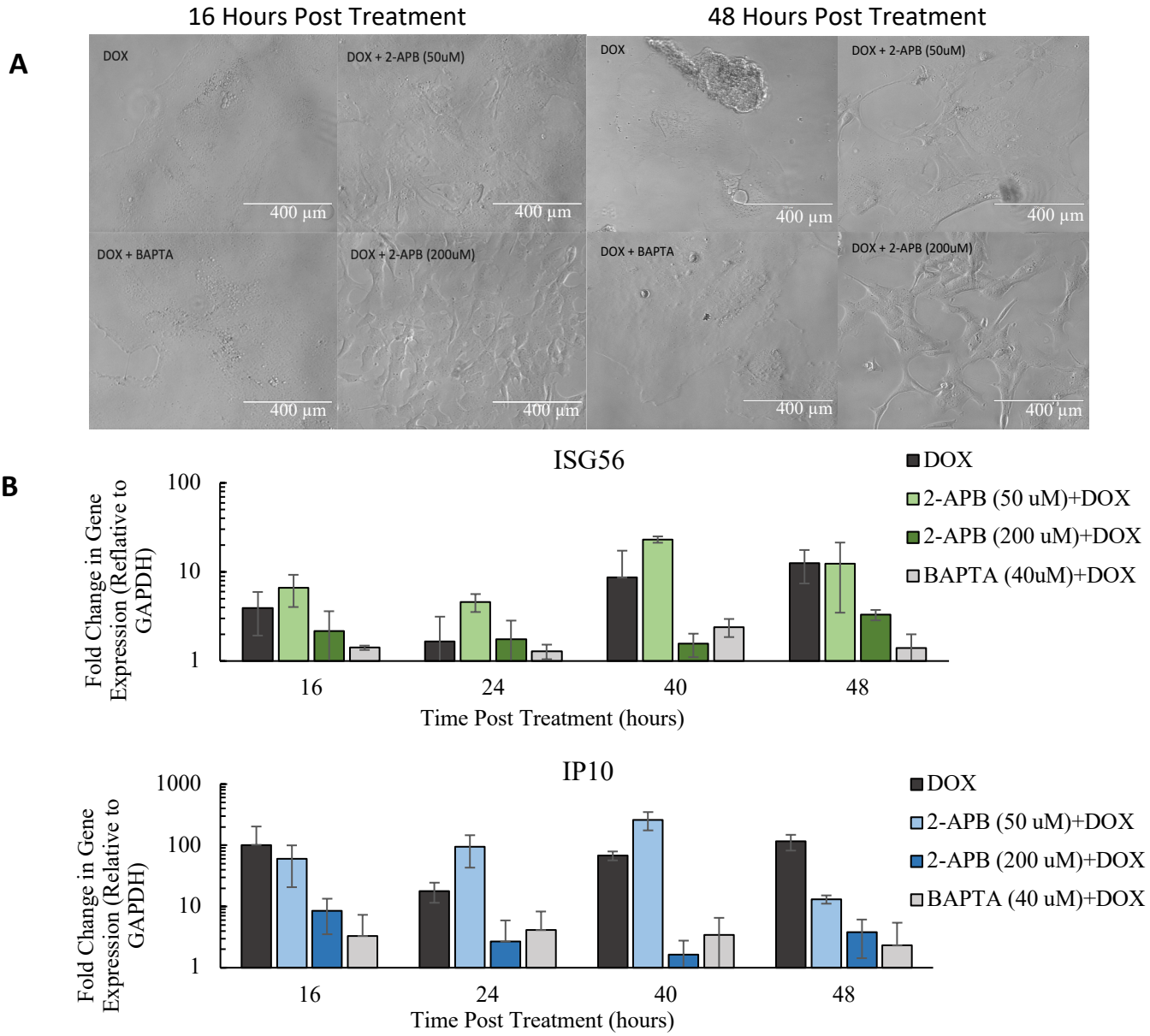


**Figure 11.** Inhibition of calcium signalling impacts p14 fusion capacity and impairs subsequent antiviral response. p14 expression was induced with 0.01 ug/ml doxycycline. Calcium inhibiting drugs were administered simultaneously at a concentration of 40 µM for BAPTA and 50 µM or 200 µM for 2-APB. **A)** The morphology of the cells was monitored for syncytia formation up to 48 post treatment. 200 µM 2-APB prevented syncytia formation, while 50 µM 2-APB and 40 µM BAPTA did not. Scale bars indicate a size of 400 µm. **B)** Changes in ISG expression levels were monitored by RT-qPCR. 200 µM 2-APB and BAPTA treatment significantly impaired the typical ISG upregulation seen in response to p14 expression and subsequent cell-cell fusion. The fold change in gene expression of each sample was calculated relative to wild type THF cells that experienced the same drug treatment. The standard deviation was calculated across three biological replicates.

# Appendix 2: Supplementary Data

## Optimizing the p14 Inducible Cell System

The initial experiment done to test for ISG upregulation in p14 expressing cells showed low levels of ISG upregulation. Thus, we attempted to optimize the p14-inducible cell system, such that ISG upregulation is maximized to facilitate comparisons in future experiments. The amount of p14 being expressed and the cell density were two factors that were predicted to contribute to the ISG response, thus we tested how various doxycycline concentrations and cell densities influence the magnitude of ISG upregulation.

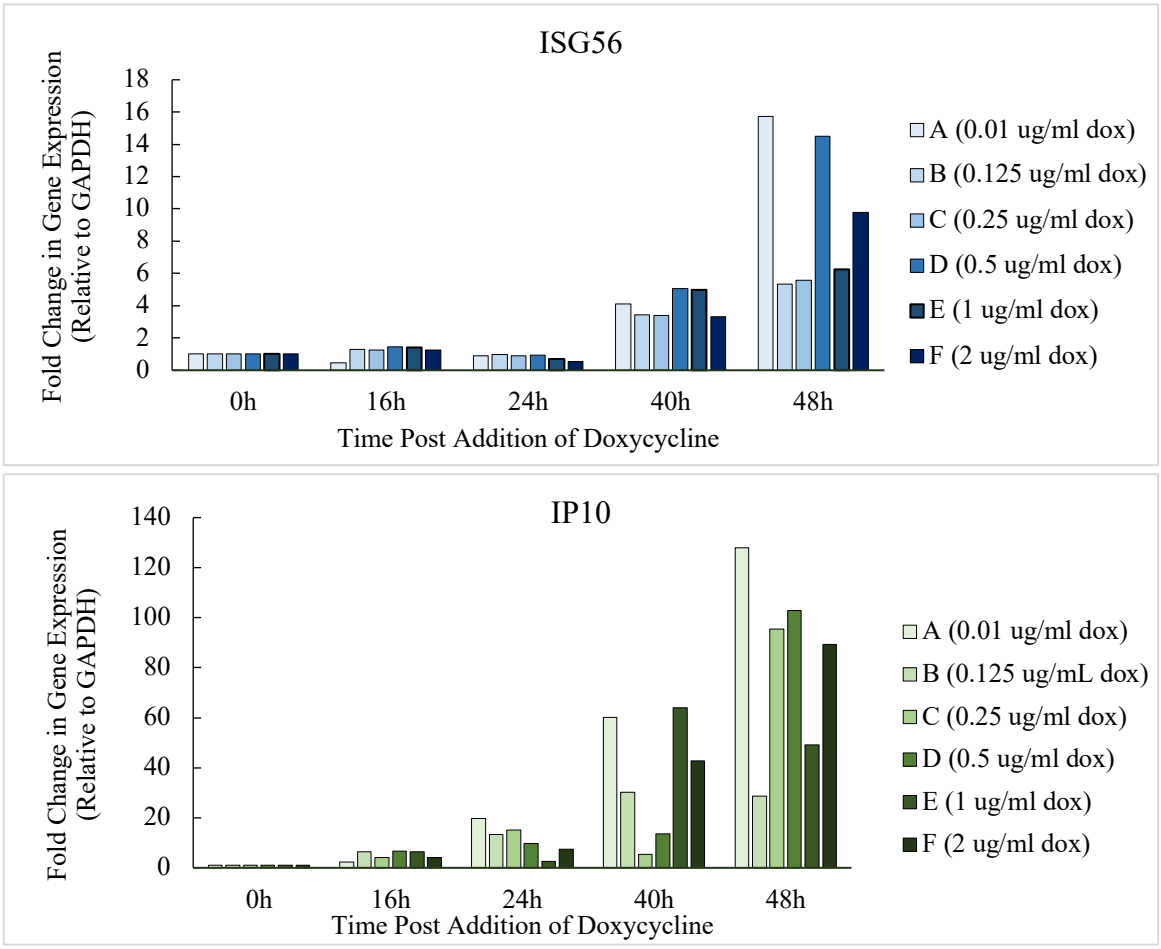


**Figure 12.** The amount of p14 expression does not correlate with the magnitude of ISG response. Contrary to expectation, treating cell with higher doxycycline concentrations to enhance p14 expression did not increase the magnitude of the ISG response, thus the lowest concentration of 0.01 μg/mL was used in all future experiments to induce p14 expression.

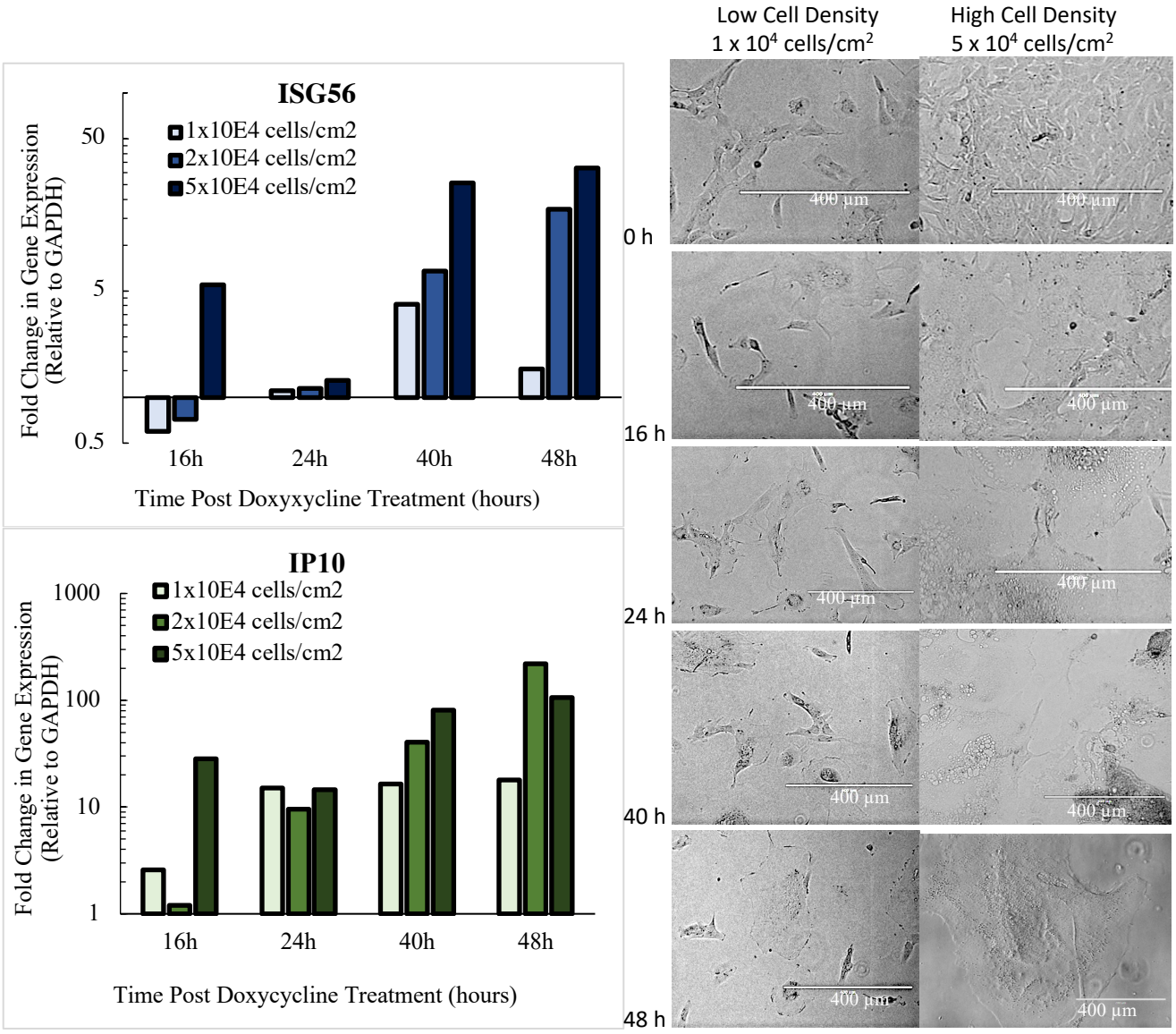


**Figure 13.** The magnitude of ISG upregulation is cell density dependent. Cell were seeded at varying density (from a low of $1x10^4$ cells/cm$^2$ to a high of $5x10^5$ cells/cm$^2$) and treated with 0.01 µg/mL doxycycline for 16 to 48 hours. Changes in ISG expression levels relative to untreated cells were measured by RT-qPCR. The magnitude of the ISG response increased with increased cell density. Scale bars indicate a size of 400 µm.

These optimization experiments illustrated that the overall trend of ISG upregulation remains the same regardless of doxycycline concentration, and the magnitude of the response could not be increased with higher doxycycline concentrations, which should correspond to higher levels of p14 expression (Figure 13). However, the magnitude of the ISG response did appear to depend on cell density, which correlates to the amount of cell-cell fusion, with stronger responses occurring at higher cell density (Figure 14). This suggests that the ISG response is associated with the extent of cell-cell fusion and syncytiogenesis, supporting the idea that p14-mediated membrane perturbations trigger an antiviral response in cells. However, cell density can also affect paracrine signalling of IFN, as IFN is more potent at higher cell density where IFN can reach and signal neighbouring cells more readily.

## Role of RLRs: Endogenous p14

In attempt to investigate the role of RLRs in the p14-mediated antiviral response, THF cells deficient in both RIG-I and MDA5 were transduced to express p14 under a tetracycline inducible promoter. However, these cells did not form large syncytia when p14 expression was induced as seen previously with p14-THF , p14- IRF3$^{-/-}$ and p14-STING$^{-/-}$ THF cells despite the presence of significant p14 transcript levels in the cells (Figure 15A). This could simply be a result of technical issues such as clonal variability from the production of the RIG-I/MDA5$^{-/-}$ THF cells. Alternatively, this could imply a novel role for RIG-I and/or MDA5 in the process of syncytia formation. RIG-I has been shown to associate with actin-rich membrane ruffles of cytoskeleton and play a role in cell migration, which requires actin polymerization and depolymerization[126]. Additionally RIG-I deficient macrophages have impaired phagocytosis and actin polymerization[127]. Since syncytia formation requires extensive actin remodeling, cells deficient in RIG-I may not be able to execute the required actin reorganization for effective pore expansion.

p14 expression in RIG-I/MDA5$^{-/-}$ cells did not provide antiviral protection from VSV-GFP (Figure 15B). This can be attributed to either the lack of cell fusion or the RLR deficiency, thus we cannot conclude whether RLRs are required for the endogenous p14 antiviral response. Knock-down or knock-out of RLRs or the downstream adaptor MAVS in wild type p14-THF cells is an alternative approach that may yield fusion-competent p14-THF RIG-I/MDA5$^{-/-}$ cells and allow for distinction between the two effects.

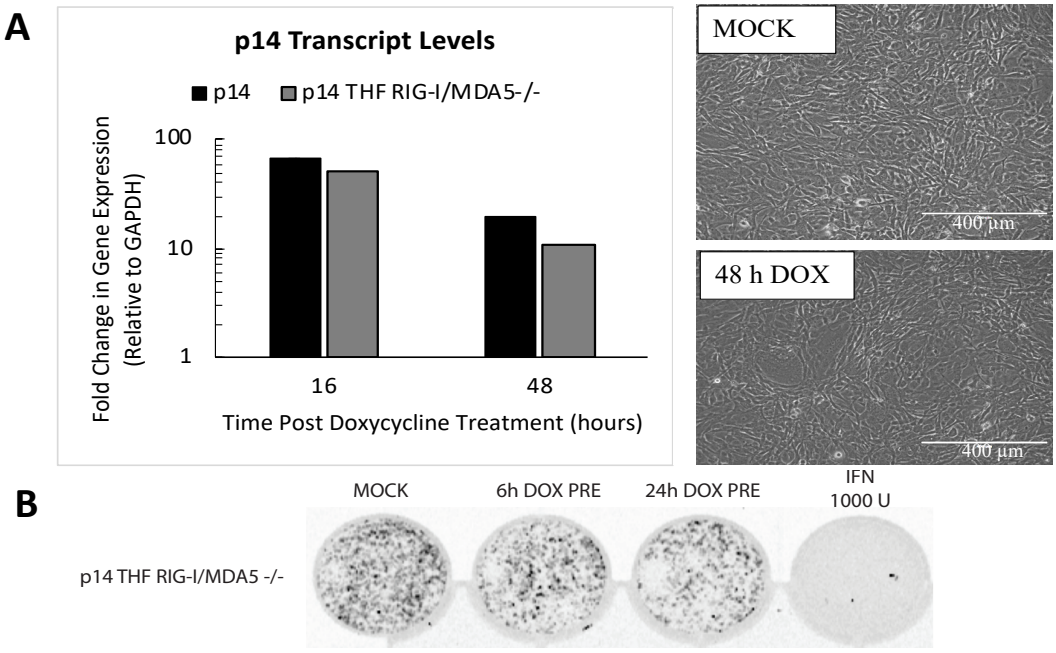


**Figure 14.** RLR knock-out p14-THF cells produce good transcript copy number despite their diminished ability to form syncytia. **A)** Cells were treated with 0.01 µg/mL doxycycline for 16 or 48 hours and the fold change in p14 transcript expression was measured relative to each cell type's respective mock treated sample. All cell types expressed similar amounts of p14, but no syncytial cells were visible. **B)** Cells were pre-treated with 0.01 µg/mL doxycycline for 6 or 24 hours, then challenged with VSV-GFP. No antiviral response was observed.

## mTOR Activation in p14 Syncytial Cells

We've seen that endogenous p14 expression and syncytia formation can restrict virus replication in an IFN independent manner (Figures 7 and 8). This suggests that other mechanisms may be involved in reducing virus replication. Possible factors include senescence, apoptotic, autophagic pathways or inhibition of protein translation. mTOR and its associated pathways are involved in cell growth, proliferation, motility, survival, autophagy, protein synthesis, and transcription[128]. Thus, the activation state of key players in the mTOR pathway can help identify what pathways may be contributing to the antiviral state of syncytial cells. p70-S6 kinase is a serine/threonine kinase downstream of the PI3K/AKT/mTOR pathway and targets the S6 ribosomal protein[114,115]. Phosphorylation of p70-S6 kinase induces protein synthesis at the ribosome and is used as a marker of mTOR activation. Phosphorylation of p70-S6 kinase correlates to autophagy inhibition and protein translation initiation[128]. We looked at the phosphorylation state of p70-S6 kinase in p14 expressing syncytial cells to see whether mTOR associated pathways may be activated or inhibited. p70-S6K was activated in p14 syncytial cells suggesting active protein translation and inhibition of autophagy; however, the mechanisms of how p70 is activated in p14 syncytial cells has not yet been investigated and the association between this pathway and STING signalling, if any, remains unknown in this system.

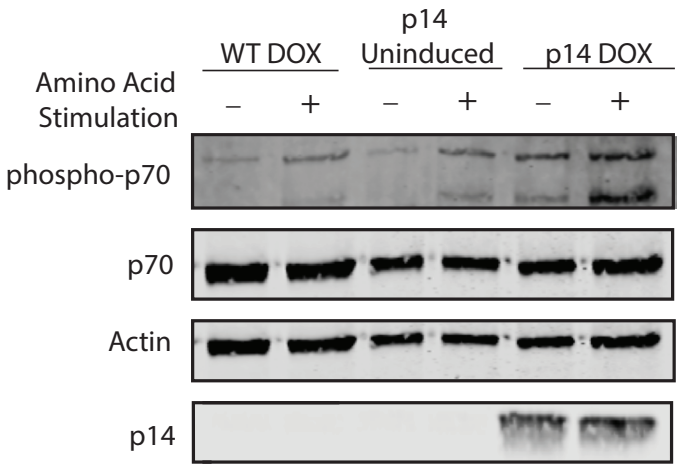


**Figure 15.** p70-S6 kinase is activated in p14-induced syncytial cells. p14-THF cells were treated with 0.01μg/mL doxycycline for 24 hours. Cells were then placed under serum-free conditions for 2 hours, which served to dephosphorylate p70SK6 as cells enter a stable G0 state. Subsequent stimulation with essential amino acids rapidly induced p70S6K activation through phosphorylation by mTORC1, which is activated via the PI3K pathway. Persistent activation of p70SK6 was observed in syncytial cells.

## References


(1) Hare, D.; Mossman, K. L. Novel Paradigms of Innate Immune Sensing of Viral Infections. *Cytokine* **2013**, *63* (3), 219–224. https://doi.org/10.1016/j.cyto.2013.06.001.

(2) Liu, Y.-P.; Zeng, L.; Tian, A.; Bomkamp, A.; Rivera, D.; Gutman, D.; Barber, G. N.; Olson, J. K.; Smith, J. A. Endoplasmic Reticulum Stress Regulates the Innate Immunity Critical Transcription Factor IRF3. *J.I.* **2012**, *189* (9), 4630–4639. https://doi.org/10.4049/jimmunol.1102737.

(3) Holm, C. K.; Jensen, S. B.; Jakobsen, M. R.; Cheshenko, N.; Horan, K. A.; Moeller, H. B.; Gonzalez-Dosal, R.; Rasmussen, S. B.; Christensen, M. H.; Yarovinsky, T. O.; Rixon, F. J.; Herold, B. C.; Fitzgerald, K. A.; Paludan, S. R. Virus-Cell Fusion as a Trigger of Innate Immunity Dependent on the Adaptor STING. *Nat. Immunol.* **2012**, *13* (8), 737–743. https://doi.org/10.1038/ni.2350.

(4) Alberts, B.; Johnson, A.; Lewis, J.; Raff, M.; Roberts, K.; Walter, P. Innate Immunity. *Molecular Biology of the Cell. 4th edition* **2002**.

(5) Kawai, T.; Akira, S. The Roles of TLRs, RLRs and NLRs in Pathogen Recognition. *International Immunology* **2009**, *21* (4), 317–337. https://doi.org/10.1093/intimm/dxp017.

(6) Koyama, S.; Ishii, K. J.; Coban, C.; Akira, S. Innate Immune Response to Viral Infection. *Cytokine* **2008**, *43* (3), 336–341. https://doi.org/10.1016/j.cyto.2008.07.009.

(7) Levy, D. E.; Marié, I. J.; Durbin, J. E. Induction and Function of Type I and III Interferon in Response to Viral Infection. *Current Opinion in Virology* **2011**, *1* (6), 476–486. https://doi.org/10.1016/j.coviro.2011.11.001.

(8) Sato, M.; Suemori, H.; Hata, N.; Asagiri, M.; Ogasawara, K.; Nakao, K.; Nakaya, T.; Katsuki, M.; Noguchi, S.; Tanaka, N.; Taniguchi, T. Distinct and Essential Roles of Transcription Factors IRF-3 and IRF-7 in Response to Viruses for IFN-␣/␤ Gene Induction. 10.

(9) Stetson, D. B.; Medzhitov, R. Type I Interferons in Host Defense. *Immunity* **2006**, *25* (3), 373–381. https://doi.org/10.1016/j.immuni.2006.08.007.

(10) Kotenko, S. V.; Gallagher, G.; Baurin, V. V.; Lewis-Antes, A.; Shen, M.; Shah, N. K.; Langer, J. A.; Sheikh, F.; Dickensheets, H.; Donnelly, R. P. IFN-λs Mediate Antiviral Protection through a Distinct Class II Cytokine Receptor Complex. *Nat Immunol* **2003**, *4* (1), 69–77. https://doi.org/10.1038/ni875.

(11) Hopfner, K.-P.; Hornung, V. Molecular Mechanisms and Cellular Functions of CGAS–STING Signalling. *Nat Rev Mol Cell Biol* **2020**, *21* (9), 501–521. https://doi.org/10.1038/s41580-020-0244-x.

(12) Chen, Q.; Sun, L.; Chen, Z. J. Regulation and Function of the CGAS–STING Pathway of Cytosolic DNA Sensing. *Nat Immunol* **2016**, *17* (10), 1142–1149. https://doi.org/10.1038/ni.3558.

(13) Zheng, J.; Mo, J.; Zhu, T.; Zhuo, W.; Yi, Y.; Hu, S.; Yin, J.; Zhang, W.; Zhou, H.; Liu, Z. Comprehensive Elaboration of the CGAS-STING Signaling Axis in Cancer Development and Immunotherapy. *Molecular Cancer* **2020**, *19* (1), 133. https://doi.org/10.1186/s12943-020-01250-1.

(14) Srikanth, S.; Woo, J. S.; Wu, B.; El-Sherbiny, Y. M.; Leung, J.; Chupradit, K.; Rice, L.; Seo, G. J.; Calmettes, G.; Ramakrishna, C.; Cantin, E.; An, D. S.; Sun, R.; Wu, T.-T.; Jung, J. U.; Savic, S.; Gwack, Y. The Ca(2+) Sensor STIM1 Regulates the Type I

Interferon Response by Retaining the Signaling Adaptor STING at the Endoplasmic Reticulum. *Nature Immunology* **2019**, *20*, 152–162.
(15) Wu, J.; Yan, N. STIM1 Moonlights as an Anchor for STING. *Nat Immunol* **2019**, *20* (2), 112–114. https://doi.org/10.1038/s41590-018-0300-2.
(16) Ablasser, A.; Schmid-Burgk, J. L.; Hemmerling, I.; Horvath, G. L.; Schmidt, T.; Latz, E.; Hornung, V. Cell Intrinsic Immunity Spreads to Bystander Cells via the Intercellular Transfer of CGAMP. *Nature* **2013**, *503* (7477), 530–534. https://doi.org/10.1038/nature12640.
(17) Li, T.; Chen, Z. J. The CGAS-CGAMP-STING Pathway Connects DNA Damage to Inflammation, Senescence, and Cancer. *J Exp Med* **2018**, *215* (5), 1287–1299. https://doi.org/10.1084/jem.20180139.
(18) Hare, D. N.; Collins, S. E.; Mukherjee, S.; Loo, Y.-M.; Gale, M.; Janssen, L. J.; Mossman, K. L. Membrane Perturbation-Associated Ca $^{2+}$ Signaling and Incoming Genome Sensing Are Required for the Host Response to Low-Level Enveloped Virus Particle Entry. *J. Virol.* **2016**, *90* (6), 3018–3027. https://doi.org/10.1128/JVI.02642-15.
(19) Hwang, I.; Uchida, H.; Dai, Z.; Li, F.; Sanchez, T.; Locasale, J. W.; Cantley, L. C.; Zheng, H.; Paik, J. Cellular Stress Signaling Activates Type-I IFN Response through FOXO3-Regulated Lamin Posttranslational Modification. *Nat Commun* **2021**, *12* (1), 1–14. https://doi.org/10.1038/s41467-020-20839-0.
(20) EGFR-Mediated Tyrosine Phosphorylation of STING Determines Its Trafficking Route and Cellular Innate Immunity Functions. *The EMBO Journal* **2020**, *39* (22), e104106. https://doi.org/10.15252/embj.2019104106.
(21) Wu, J.; Chen, Y.-J.; Dobbs, N.; Sakai, T.; Liou, J.; Miner, J. J.; Yan, N. STING-Mediated Disruption of Calcium Homeostasis Chronically Activates ER Stress and Primes T Cell Death. *Journal of Experimental Medicine* **2019**, *216* (4), 867–883. https://doi.org/10.1084/jem.20182192.
(22) Tao, L.; Lemoff, A.; Wang, G.; Zarek, C.; Lowe, A.; Yan, N.; Reese, T. A. Reactive Oxygen Species Oxidize STING and Suppress Interferon Production. *eLife* **2020**, *9*, e57837. https://doi.org/10.7554/eLife.57837.
(23) Schlee, M.; Hartmann, G. Discriminating Self from Non-Self in Nucleic Acid Sensing. *Nat Rev Immunol* **2016**, *16* (9), 566–580. https://doi.org/10.1038/nri.2016.78.
(24) Malathi, K.; Dong, B.; Gale, M.; Silverman, R. H. Small Self-RNA Generated by RNase L Amplifies Antiviral Innate Immunity. *Nature* **2007**, *448* (7155), 816–819. https://doi.org/10.1038/nature06042.
(25) Lan, Y. Y.; Londoño, D.; Bouley, R.; Rooney, M. S.; Hacohen, N. Dnase2a Deficiency Uncovers Lysosomal Clearance of Damaged Nuclear DNA via Autophagy. *Cell Rep* **2014**, *9* (1), 180–192. https://doi.org/10.1016/j.celrep.2014.08.074.
(26) Phosphorylation and chromatin tethering prevent cGAS activation during mitosis | Science https://science.sciencemag.org/content/371/6535/eabc5386?rss=1 (accessed 2021 -07 -15).
(27) A Toll-like receptor recognizes bacterial DNA - PubMed https://pubmed-ncbi-nlm-nih-gov.libaccess.lib.mcmaster.ca/11130078/?dopt=Abstract (accessed 2021 -08 -09).
(28) Gehrke, N.; Mertens, C.; Zillinger, T.; Wenzel, J.; Bald, T.; Zahn, S.; Tüting, T.; Hartmann, G.; Barchet, W. Oxidative Damage of DNA Confers Resistance to Cytosolic Nuclease TREX1 Degradation and Potentiates STING-Dependent Immune Sensing. *Immunity* **2013**, *39* (3), 482–495. https://doi.org/10.1016/j.immuni.2013.08.004.

(29) Luthra, P.; Sun, D.; Silverman, R. H.; He, B. Activation of IFN-β Expression by a Viral MRNA through RNase L and MDA5. *Proc Natl Acad Sci U S A* **2011**, *108* (5), 2118–2123. https://doi.org/10.1073/pnas.1012409108.
(30) Benitez, A. A.; Panis, M.; Xue, J.; Varble, A.; Shim, J. V.; Frick, A. L.; López, C. B.; Sachs, D.; tenOever, B. R. In Vivo RNAi Screening Identifies MDA5 as a Significant Contributor to the Cellular Defense against Influenza A Virus. *Cell Rep* **2015**, *11* (11), 1714–1726. https://doi.org/10.1016/j.celrep.2015.05.032.
(31) Marques, J. T.; Devosse, T.; Wang, D.; Zamanian-Daryoush, M.; Serbinowski, P.; Hartmann, R.; Fujita, T.; Behlke, M. A.; Williams, B. R. G. A Structural Basis for Discriminating between Self and Nonself Double-Stranded RNAs in Mammalian Cells. *Nat Biotechnol* **2006**, *24* (5), 559–565. https://doi.org/10.1038/nbt1205.
(32) Goubau, D.; Schlee, M.; Deddouche, S.; Pruijssers, A. J.; Zillinger, T.; Goldeck, M.; Schuberth, C.; Van der Veen, A. G.; Fujimura, T.; Rehwinkel, J.; Iskarpatyoti, J. A.; Barchet, W.; Ludwig, J.; Dermody, T. S.; Hartmann, G.; Reis e Sousa, C. Antiviral Immunity via RIG-I-Mediated Recognition of RNA Bearing 5'-Diphosphates. *Nature* **2014**, *514* (7522), 372–375. https://doi.org/10.1038/nature13590.
(33) Nallagatla, S. R.; Hwang, J.; Toroney, R.; Zheng, X.; Cameron, C. E.; Bevilacqua, P. C. 5'-Triphosphate-Dependent Activation of PKR by RNAs with Short Stem-Loops. *Science* **2007**, *318* (5855), 1455–1458. https://doi.org/10.1126/science.1147347.
(34) Eigenbrod, T.; Dalpke, A. H. Bacterial RNA: An Underestimated Stimulus for Innate Immune Responses. *J Immunol* **2015**, *195* (2), 411–418. https://doi.org/10.4049/jimmunol.1500530.
(35) Devarkar, S. C.; Wang, C.; Miller, M. T.; Ramanathan, A.; Jiang, F.; Khan, A. G.; Patel, S. S.; Marcotrigiano, J. Structural Basis for M7G Recognition and 2'-O-Methyl Discrimination in Capped RNAs by the Innate Immune Receptor RIG-I. *Proc Natl Acad Sci U S A* **2016**, *113* (3), 596–601. https://doi.org/10.1073/pnas.1515152113.
(36) Hyde, J. L.; Diamond, M. S. Innate Immune Restriction and Antagonism of Viral RNA Lacking 2′-O Methylation. *Virology* **2015**, *479–480*, 66–74. https://doi.org/10.1016/j.virol.2015.01.019.
(37) Lin, F.; Tang, Y.-D.; Zheng, C. The Crosstalk between DNA Damage Response Components and DNA-Sensing Innate Immune Signaling Pathways. *International Reviews of Immunology* **2021**, *0* (0), 1–9. https://doi.org/10.1080/08830185.2021.1898605.
(38) Stucki, M.; Clapperton, J. A.; Mohammad, D.; Yaffe, M. B.; Smerdon, S. J.; Jackson, S. P. MDC1 Directly Binds Phosphorylated Histone H2AX to Regulate Cellular Responses to DNA Double-Strand Breaks. *Cell* **2005**, *123* (7), 1213–1226. https://doi.org/10.1016/j.cell.2005.09.038.
(39) Kitagawa, R.; Bakkenist, C. J.; McKinnon, P. J.; Kastan, M. B. Phosphorylation of SMC1 Is a Critical Downstream Event in the ATM-NBS1-BRCA1 Pathway. *Genes Dev* **2004**, *18* (12), 1423–1438. https://doi.org/10.1101/gad.1200304.
(40) Du, M.; Chen, Z. J. DNA-Induced Liquid Phase Condensation of CGAS Activates Innate Immune Signaling. *Science* **2018**, *361* (6403), 704–709. https://doi.org/10.1126/science.aat1022.
(41) Harding, S. M.; Benci, J. L.; Irianto, J.; Discher, D. E.; Minn, A. J.; Greenberg, R. A. Mitotic Progression Following DNA Damage Enables Pattern Recognition within Micronuclei. *Nature* **2017**, *548* (7668), 466–470. https://doi.org/10.1038/nature23470.

(42) Ku, J. W. K.; Chen, Y.; Lim, B. J. W.; Gasser, S.; Crasta, K. C.; Gan, Y.-H. Bacterial-Induced Cell Fusion Is a Danger Signal Triggering CGAS–STING Pathway via Micronuclei Formation. *PNAS* **2020**, *117* (27), 15923–15934. https://doi.org/10.1073/pnas.2006908117.
(43) Zahid, A.; Ismail, H.; Li, B.; Jin, T. Molecular and Structural Basis of DNA Sensors in Antiviral Innate Immunity. *Front. Immunol.* **2020**, *0*. https://doi.org/10.3389/fimmu.2020.613039.
(44) Karpova, A. Y.; Trost, M.; Murray, J. M.; Cantley, L. C.; Howley, P. M. Interferon Regulatory Factor-3 Is an in Vivo Target of DNA-PK. *PNAS* **2002**, *99* (5), 2818–2823. https://doi.org/10.1073/pnas.052713899.
(45) Ferguson, B. J.; Mansur, D. S.; Peters, N. E.; Ren, H.; Smith, G. L. DNA-PK Is a DNA Sensor for IRF-3-Dependent Innate Immunity. *Elife* **2012**, *1*, e00047. https://doi.org/10.7554/eLife.00047.
(46) Louten, J. Virus Structure and Classification. *Essential Human Virology* **2016**, 19–29. https://doi.org/10.1016/B978-0-12-800947-5.00002-8.
(47) Leroy, H.; Han, M.; Woottum, M.; Bracq, L.; Bouchet, J.; Xie, M.; Benichou, S. Virus-Mediated Cell-Cell Fusion. *IJMS* **2020**, *21* (24), 9644. https://doi.org/10.3390/ijms21249644.
(48) White, J. M.; Delos, S. E.; Brecher, M.; Schornberg, K. Structures and Mechanisms of Viral Membrane Fusion Proteins. *Crit Rev Biochem Mol Biol* **2008**, *43* (3), 189–219. https://doi.org/10.1080/10409230802058320.
(49) Blank, H.; Burgoon, C. F.; Baldridge, G. D.; McCarthy, P. L.; Urbach, F. CYTOLOGIC SMEARS IN DIAGNOSIS OF HERPES SIMPLEX, HERPES ZOSTER, AND VARICELLA. *Journal of the American Medical Association* **1951**, *146* (15), 1410–1412. https://doi.org/10.1001/jama.1951.63670150005012b.
(50) Pritt, B. S.; Aubry, M. C. Histopathology of Viral Infections of the Lung. *Semin Diagn Pathol* **2017**, *34* (6), 510–517. https://doi.org/10.1053/j.semdp.2017.06.005.
(51) WHEELER, C. E.; Canby, C. M. Herpes Simplex Virus: Characteristics of a Strain Which Produces Unusually Large Multinucleated Giant Cells in Tissue Culture. *Archives of Dermatology* **1960**, *82* (3), 391–399. https://doi.org/10.1001/archderm.1960.01580030085011.
(52) Galitska, G.; Biolatti, M.; De Andrea, M.; Leone, A.; Coscia, A.; Bertolotti, L.; Ala, U.; Bertino, E.; Dell'Oste, V.; Landolfo, S. Biological Relevance of Cytomegalovirus Genetic Variability in Congenitally and Postnatally Infected Children. *Journal of Clinical Virology* **2018**, *108*, 132–140. https://doi.org/10.1016/j.jcv.2018.09.019.
(53) Atanasiu, D.; Whitbeck, J. C.; Cairns, T. M.; Reilly, B.; Cohen, G. H.; Eisenberg, R. J. Bimolecular Complementation Reveals That Glycoproteins GB and GH/GL of Herpes Simplex Virus Interact with Each Other during Cell Fusion. *PNAS* **2007**, *104* (47), 18718–18723. https://doi.org/10.1073/pnas.0707452104.
(54) Beitia Ortiz de Zarate, I.; Cantero-Aguilar, L.; Longo, M.; Berlioz-Torrent, C.; Rozenberg, F. Contribution of Endocytic Motifs in the Cytoplasmic Tail of Herpes Simplex Virus Type 1 Glycoprotein B to Virus Replication and Cell-Cell Fusion. *J Virol* **2007**, *81* (24), 13889–13903. https://doi.org/10.1128/JVI.01231-07.
(55) Engel, J. P.; Boyer, E. P.; Goodman, J. L. Two Novel Single Amino Acid Syncytial Mutations in the Carboxy Terminus of Glycoprotein B of Herpes Simplex Virus Type 1

Confer a Unique Pathogenic Phenotype. *Virology* **1993**, *192* (1), 112–120. https://doi.org/10.1006/viro.1993.1013.

(56) Cai, W. H.; Gu, B.; Person, S. Role of Glycoprotein B of Herpes Simplex Virus Type 1 in Viral Entry and Cell Fusion. *Journal of Virology* **1988**, *62* (8), 2596–2604. https://doi.org/10.1128/jvi.62.8.2596-2604.1988.

(57) Ludlow, M.; McQuaid, S.; Milner, D.; Swart, R. L. de; Duprex, W. P. Pathological Consequences of Systemic Measles Virus Infection. *The Journal of Pathology* **2015**, *235* (2), 253–265. https://doi.org/10.1002/path.4457.

(58) Osunkoya, B. O.; Ukaejiofo, E. O.; Ajayi, O.; Akinyemi, A. A. Evidence That Circulating Lymphocytes Act as Vehicles or Viraemia in Measles. *West Afr J Med* **1990**, *9* (1), 35–39.

(59) Johnson, J. E.; Gonzales, R. A.; Olson, S. J.; Wright, P. F.; Graham, B. S. The Histopathology of Fatal Untreated Human Respiratory Syncytial Virus Infection. *Mod Pathol* **2007**, *20* (1), 108–119. https://doi.org/10.1038/modpathol.3800725.

(60) Navaratnarajah, C. K.; Leonard, V. H. J.; Cattaneo, R. Measles Virus Glycoprotein Complex Assembly, Receptor Attachment, and Cell Entry. In *Measles: History and Basic Biology*; Griffin, D. E., Oldstone, M. B. A., Eds.; Current Topics in Microbiology and Immunology; Springer: Berlin, Heidelberg, 2009; pp 59–76. https://doi.org/10.1007/978-3-540-70523-9_4.

(61) Russell, C. J.; Luque, L. E. The Structural Basis of Paramyxovirus Invasion. *Trends in Microbiology* **2006**, *14* (6), 243–246. https://doi.org/10.1016/j.tim.2006.04.004.

(62) Buchrieser, J.; Dufloo, J.; Hubert, M.; Monel, B.; Planas, D.; Rajah, M. M.; Planchais, C.; Porrot, F.; Guivel-Benhassine, F.; Van der Werf, S.; Casartelli, N.; Mouquet, H.; Bruel, T.; Schwartz, O. Syncytia Formation by SARS-CoV-2-Infected Cells. *The EMBO Journal* **2020**, *39* (23), e106267. https://doi.org/10.15252/embj.2020106267.

(63) SARS-CoV-2 Requires Cholesterol for Viral Entry and Pathological Syncytia Formation | bioRxiv https://www.biorxiv.org/content/10.1101/2020.12.14.422737v1.full (accessed 2021 -02 -13).

(64) Syncytia formation during SARS-CoV-2 lung infection: a disastrous unity to eliminate lymphocytes | Cell Death & Differentiation https://www.nature.com/articles/s41418-021-00795-y (accessed 2021 -06 -16).

(65) Sainz, B.; Rausch, J. M.; Gallaher, W. R.; Garry, R. F.; Wimley, W. C. Identification and Characterization of the Putative Fusion Peptide of the Severe Acute Respiratory Syndrome-Associated Coronavirus Spike Protein. *J Virol* **2005**, *79* (11), 7195–7206. https://doi.org/10.1128/JVI.79.11.7195-7206.2005.

(66) Compton, A. A.; Schwartz, O. They Might Be Giants: Does Syncytium Formation Sink or Spread HIV Infection? *PLOS Pathogens* **2017**, *13* (2), e1006099. https://doi.org/10.1371/journal.ppat.1006099.

(67) Murooka, T. T.; Deruaz, M.; Marangoni, F.; Vrbanac, V. D.; Seung, E.; von Andrian, U. H.; Tager, A. M.; Luster, A. D.; Mempel, T. R. HIV-Infected T Cells Are Migratory Vehicles for Viral Dissemination. *Nature* **2012**, *490* (7419), 283–287. https://doi.org/10.1038/nature11398.

(68) Orenstein, J. M. In Vivo Cytolysis and Fusion of Human Immunodeficiency Virus Type 1-Infected Lymphocytes in Lymphoid Tissue. *The Journal of Infectious Diseases* **2000**, *182* (1), 338–342. https://doi.org/10.1086/315640.

(69) Gower, T. L.; Pastey, M. K.; Peeples, M. E.; Collins, P. L.; McCurdy, L. H.; Hart, T. K.; Guth, A.; Johnson, T. R.; Graham, B. S. RhoA Signaling Is Required for Respiratory

Syncytial Virus-Induced Syncytium Formation and Filamentous Virion Morphology. *Journal of Virology* **2005**, *79* (9), 5326–5336. https://doi.org/10.1128/JVI.79.9.5326-5336.2005.

(70) Bestle, D.; Heindl, M. R.; Limburg, H.; Van Lam van, T.; Pilgram, O.; Moulton, H.; Stein, D. A.; Hardes, K.; Eickmann, M.; Dolnik, O.; Rohde, C.; Klenk, H.-D.; Garten, W.; Steinmetzer, T.; Böttcher-Friebertshäuser, E. TMPRSS2 and Furin Are Both Essential for Proteolytic Activation of SARS-CoV-2 in Human Airway Cells. *Life Sci Alliance* **2020**, *3* (9). https://doi.org/10.26508/lsa.202000786.

(71) Ciechonska, M.; Duncan, R. Reovirus FAST Proteins: Virus-Encoded Cellular Fusogens. *Trends in Microbiology* **2014**, *22* (12), 715–724. https://doi.org/10.1016/j.tim.2014.08.005.

(72) Salsman, J.; Top, D.; Barry, C.; Duncan, R. A Virus-Encoded Cell–Cell Fusion Machine Dependent on Surrogate Adhesins. *PLOS Pathogens* **2008**, *4* (3), e1000016. https://doi.org/10.1371/journal.ppat.1000016.

(73) Ciechonska, M.; Key, T.; Duncan, R. Efficient Reovirus- and Measles Virus-Mediated Pore Expansion during Syncytium Formation Is Dependent on Annexin A1 and Intracellular Calcium. *Journal of Virology* **2014**, *88* (11), 6137–6147. https://doi.org/10.1128/JVI.00121-14.

(74) Yamanaka, A.; Iwakiri, A.; Yoshikawa, T.; Sakai, K.; Singh, H.; Himeji, D.; Kikuchi, I.; Ueda, A.; Yamamoto, S.; Miura, M.; Shioyama, Y.; Kawano, K.; Nagaishi, T.; Saito, M.; Minomo, M.; Iwamoto, N.; Hidaka, Y.; Sohma, H.; Kobayashi, T.; Kanai, Y.; Kawagishi, T.; Nagata, N.; Fukushi, S.; Mizutani, T.; Tani, H.; Taniguchi, S.; Fukuma, A.; Shimojima, M.; Kurane, I.; Kageyama, T.; Odagiri, T.; Saijo, M.; Morikawa, S. Imported Case of Acute Respiratory Tract Infection Associated with a Member of Species Nelson Bay Orthoreovirus. *PLOS ONE* **2014**, *9* (3), e92777. https://doi.org/10.1371/journal.pone.0092777.

(75) Chua, K. B.; Voon, K.; Yu, M.; Keniscope, C.; Rasid, K. A.; Wang, L.-F. Investigation of a Potential Zoonotic Transmission of Orthoreovirus Associated with Acute Influenza-Like Illness in an Adult Patient. *PLOS ONE* **2011**, *6* (10), e25434. https://doi.org/10.1371/journal.pone.0025434.

(76) Chua, K. B.; Voon, K.; Crameri, G.; Tan, H. S.; Rosli, J.; McEachern, J. A.; Suluraju, S.; Yu, M.; Wang, L.-F. Identification and Characterization of a New Orthoreovirus from Patients with Acute Respiratory Infections. *PLOS ONE* **2008**, *3* (11), e3803. https://doi.org/10.1371/journal.pone.0003803.

(77) Chua, K. B.; Crameri, G.; Hyatt, A.; Yu, M.; Tompang, M. R.; Rosli, J.; McEachern, J.; Crameri, S.; Kumarasamy, V.; Eaton, B. T.; Wang, L.-F. A Previously Unknown Reovirus of Bat Origin Is Associated with an Acute Respiratory Disease in Humans. *PNAS* **2007**, *104* (27), 11424–11429. https://doi.org/10.1073/pnas.0701372104.

(78) Cheng, P.; ChiShan, L.; Lai, A.; Ho, E.; Leung, P.; Chan, F.; Wong, A.; Lim, W. A Novel Reovirus Isolated from a Patient with Acute Respiratory Disease. *Journal of Clinical Virology* **2009**, *45* (1), 79–80.

(79) Gasser, A.; Möst, J. Generation of Multinucleated Giant Cells in Vitro by Culture of Human Monocytes with Mycobacterium Bovis BCG in Combination with Cytokine-Containing Supernatants. *Infect Immun* **1999**, *67* (1), 395–402. https://doi.org/10.1128/IAI.67.1.395-402.1999.

(80) Kuny, C. V.; Bowen, C. D.; Renner, D. W.; Johnston, C. M.; Szpara, M. L. In Vitro Evolution of Herpes Simplex Virus 1 (HSV-1) Reveals Selection for Syncytia and Other Minor Variants in Cell Culture. *Virus Evol* **2020**, *6* (1). https://doi.org/10.1093/ve/veaa013.
(81) Compton, A. A.; Schwartz, O. They Might Be Giants: Does Syncytium Formation Sink or Spread HIV Infection? *PLOS Pathogens* **2017**, *13* (2), e1006099. https://doi.org/10.1371/journal.ppat.1006099.
(82) Guedan, S.; Gros, A.; Cascallo, M.; Vile, R.; Mercade, E.; Alemany, R. Syncytia Formation Affects the Yield and Cytotoxicity of an Adenovirus Expressing a Fusogenic Glycoprotein at a Late Stage of Replication. *Gene Therapy* **2008**, *15* (17), 1240–1245. https://doi.org/10.1038/gt.2008.94.
(83) Dysregulated signalling pathways in innate immune cells with cystic fibrosis mutations | SpringerLink https://link.springer.com/article/10.1007/s00018-020-03540-9 (accessed 2021 -04 -06).
(84) Carletti, T.; Zakaria, M. K.; Faoro, V.; Reale, L.; Kazungu, Y.; Licastro, D.; Marcello, A. Viral Priming of Cell Intrinsic Innate Antiviral Signaling by the Unfolded Protein Response. *Nat Commun* **2019**, *10* (1), 3889. https://doi.org/10.1038/s41467-019-11663-2.
(85) Kustermans, G.; Benna, J. E.; Piette, J.; Legrand-Poels, S. Perturbation of Actin Dynamics Induces NF-KB Activation in Myelomonocytic Cells through an NADPH Oxidase-Dependent Pathway. *Biochemical Journal* **2005**, *387* (2), 531–540. https://doi.org/10.1042/BJ20041318.
(86) Collins, S. E.; Noyce, R. S.; Mossman, K. L. Innate Cellular Response to Virus Particle Entry Requires IRF3 but Not Virus Replication. *Journal of Virology* **2004**, *78* (4), 1706–1717. https://doi.org/10.1128/JVI.78.4.1706-1717.2004.
(87) Mossman, K. L.; Macgregor, P. F.; Rozmus, J. J.; Goryachev, A. B.; Edwards, A. M.; Smiley, J. R. Herpes Simplex Virus Triggers and Then Disarms a Host Antiviral Response. *Journal of Virology* **2001**, *75* (2), 750–758. https://doi.org/10.1128/JVI.75.2.750-758.2001.
(88) Paladino, P.; Cummings, D. T.; Noyce, R. S.; Mossman, K. L. The IFN-Independent Response to Virus Particle Entry Provides a First Line of Antiviral Defense That Is Independent of TLRs and Retinoic Acid-Inducible Gene I. *J Immunol* **2006**, *177* (11), 8008–8016. https://doi.org/10.4049/jimmunol.177.11.8008.
(89) Tsitoura, E.; Thomas, J.; Cuchet, D.; Thoinet, K.; Mavromara, P.; Epstein, A. L. Infection with Herpes Simplex Type 1-Based Amplicon Vectors Results in an IRF3/7-Dependent, TLR-Independent Activation of the Innate Antiviral Response in Primary Human Fibroblasts. *Journal of General Virology* **2009**, *90* (9), 2209–2220. https://doi.org/10.1099/vir.0.012203-0.
(90) Noyce, R. S.; Taylor, K.; Ciechonska, M.; Collins, S. E.; Duncan, R.; Mossman, K. L. Membrane Perturbation Elicits an IRF3-Dependent, Interferon-Independent Antiviral Response. *Journal of Virology* **2011**, *85* (20), 10926–10931. https://doi.org/10.1128/JVI.00862-11.
(91) Hare, D. N.; Baid, K.; Dvorkin-Gheva, A.; Mossman, K. L. Virus-Intrinsic Differences and Heterogeneous IRF3 Activation Influence IFN-Independent Antiviral Protection. *iScience* **2020**, *23* (12), 101864. https://doi.org/10.1016/j.isci.2020.101864.
(92) Hare, D. David Hare Ph.D Defense Thesis, 2020.

(93) Li, Z.; Michael, I. P.; Zhou, D.; Nagy, A.; Rini, J. M. Simple PiggyBac Transposon-Based Mammalian Cell Expression System for Inducible Protein Production. *Proceedings of the National Academy of Sciences* **2013**, *110* (13), 5004–5009. https://doi.org/10.1073/pnas.1218620110.

(94) Bresnahan, W. A.; Hultman, G. E.; Shenk, T. Replication of Wild-Type and Mutant Human Cytomegalovirus in Life-Extended Human Diploid Fibroblasts. *Journal of Virology* **2000**, *74* (22), 10816–10818. https://doi.org/10.1128/JVI.74.22.10816-10818.2000.

(95) Sali, T. M.; Pryke, K. M.; Abraham, J.; Liu, A.; Archer, I.; Broeckel, R.; Staverosky, J. A.; Smith, J. L.; Al-Shammari, A.; Amsler, L.; Sheridan, K.; Nilsen, A.; Streblow, D. N.; DeFilippis, V. R. Characterization of a Novel Human-Specific STING Agonist That Elicits Antiviral Activity Against Emerging Alphaviruses. *PLoS Pathog* **2015**, *11* (12), e1005324. https://doi.org/10.1371/journal.ppat.1005324.

(96) Yang, J.; Tang, X.; Nandakumar, K. S.; Cheng, K. Autophagy Induced by STING, an Unnoticed and Primordial Function of CGAS. *Cellular & Molecular Immunology* **2019**, *16* (8), 683–684. https://doi.org/10.1038/s41423-019-0240-2.

(97) STING directly activates autophagy to tune the innate immune response | Cell Death & Differentiation https://www.nature.com/articles/s41418-018-0251-z (accessed 2021 -05 -27).

(98) Wan, D.; Jiang, W.; Hao, J. Research Advances in How the CGAS-STING Pathway Controls the Cellular Inflammatory Response. *Front. Immunol.* **2020**, *0*. https://doi.org/10.3389/fimmu.2020.00615.

(99) Yamashiro, L. H.; Wilson, S. C.; Morrison, H. M.; Karalis, V.; Chung, J.-Y. J.; Chen, K. J.; Bateup, H. S.; Szpara, M. L.; Lee, A. Y.; Cox, J. S.; Vance, R. E. Interferon-Independent STING Signaling Promotes Resistance to HSV-1 in Vivo. *Nat Commun* **2020**, *11* (1), 3382. https://doi.org/10.1038/s41467-020-17156-x.

(100) Loo, T. M.; Miyata, K.; Tanaka, Y.; Takahashi, A. Cellular Senescence and Senescence-associated Secretory Phenotype via the CGAS-STING Signaling Pathway in Cancer. *Cancer Sci* **2020**, *111* (2), 304–311. https://doi.org/10.1111/cas.14266.

(101) Baz-Martínez, M.; Da Silva-Álvarez, S.; Rodríguez, E.; Guerra, J.; El Motiam, A.; Vidal, A.; García-Caballero, T.; González-Barcia, M.; Sánchez, L.; Muñoz-Fontela, C.; Collado, M.; Rivas, C. Cell Senescence Is an Antiviral Defense Mechanism. *Sci Rep* **2016**, *6*, 37007. https://doi.org/10.1038/srep37007.

(102) Herschke, F.; Plumet, S.; Duhen, T.; Azocar, O.; Druelle, J.; Laine, D.; Wild, T. F.; Rabourdin-Combe, C.; Gerlier, D.; Valentin, H. Cell-Cell Fusion Induced by Measles Virus Amplifies the Type I Interferon Response. *Journal of Virology* **2007**, *81* (23), 12859–12871. https://doi.org/10.1128/JVI.00078-07.

(103) Zhou, Z.; Zhang, X.; Lei, X.; Xiao, X.; Jiao, T.; Ma, R.; Dong, X.; Jiang, Q.; Wang, W.; Shi, Y.; Zheng, T.; Tan, Y.; Xiang, Z.; Ren, L.; Deng, T.; Jiang, Z.; Dou, Z.; Wei, W.; Wang, J. *Sensing of Cytoplasmic Chromatin by CGAS Activates Innate Immune Response in SARS-CoV-2 Infection*; preprint; In Review, 2021. https://doi.org/10.21203/rs.3.rs-235742/v1.

(104) Ku, J. W. K.; Chen, Y.; Lim, B. J. W.; Gasser, S.; Crasta, K. C.; Gan, Y.-H. Bacterial-Induced Cell Fusion Is a Danger Signal Triggering CGAS–STING Pathway via Micronuclei Formation. *PNAS* **2020**, *117* (27), 15923–15934. https://doi.org/10.1073/pnas.2006908117.

(105) Gekara, N. O. DNA Damage-Induced Immune Response: Micronuclei Provide Key Platform. *J Cell Biol* **2017**, *216* (10), 2999–3001. https://doi.org/10.1083/jcb.201708069.
(106) Torgovnick, A.; Schumacher, B. DNA Repair Mechanisms in Cancer Development and Therapy. *Front. Genet.* **2015**, *0*. https://doi.org/10.3389/fgene.2015.00157.
(107) Autophagy and DNA damage repair | SpringerLink https://link.springer.com/article/10.1007/s42764-020-00016-9 (accessed 2021 -04 -28).
(108) Reisländer, T.; Groelly, F. J.; Tarsounas, M. DNA Damage and Cancer Immunotherapy: A STING in the Tale. *Molecular Cell* **2020**, *80* (1), 21–28. https://doi.org/10.1016/j.molcel.2020.07.026.
(109) Burton, C.; Bartee, E. Syncytia Formation in Oncolytic Virotherapy. *Mol Ther Oncolytics* **2019**, *15*, 131–139. https://doi.org/10.1016/j.omto.2019.09.006.
(110) Papa, J. D.; Petryk, J.; Bell, J. C.; Parks, R. J. An Oncolytic Adenovirus Vector Expressing P14 FAST Protein Induces Widespread Syncytium Formation and Reduces Tumor Growth Rate In Vivo. *Molecular Therapy - Oncolytics* **2019**, *14*, 107–120. https://doi.org/10.1016/j.omto.2019.05.001.
(111) Le Boeuf, F.; Gebremeskel, S.; McMullen, N.; He, H.; Greenshields, A. L.; Hoskin, D. W.; Bell, J. C.; Johnston, B.; Pan, C.; Duncan, R. Reovirus FAST Protein Enhances Vesicular Stomatitis Virus Oncolytic Virotherapy in Primary and Metastatic Tumor Models. *Mol Ther Oncolytics* **2017**, *6*, 80–89. https://doi.org/10.1016/j.omto.2017.08.001.
(112) Bootman, M. D.; Bultynck, G. Fundamentals of Cellular Calcium Signaling: A Primer. *Cold Spring Harb Perspect Biol* **2019**, a038802. https://doi.org/10.1101/cshperspect.a038802.
(113) Schuster, S.; Marhl, M.; Höfer, T. Modelling of Simple and Complex Calcium Oscillations: From Single-Cell Responses to Intercellular Signalling. *European Journal of Biochemistry* **2002**, *269* (5), 1333–1355. https://doi.org/10.1046/j.0014-2956.2001.02720.x.
(114) Berridge, M. J.; Lipp, P.; Bootman, M. D. The Versatility and Universality of Calcium Signalling. *Nature Reviews Molecular Cell Biology* **2000**, *1*, 11–21.
(115) Chang-Graham, A. L.; Perry, J. L.; Strtak, A. C.; Ramachandran, N. K.; Criglar, J. M.; Philip, A. A.; Patton, J. T.; Estes, M. K.; Hyser, J. M. *Rotavirus Calcium Dysregulation Manifests as Dynamic Calcium Signaling in the Cytoplasm and Endoplasmic Reticulum*; preprint; Microbiology, 2019. https://doi.org/10.1101/627877.
(116) Bhattacharyya, M.; Karandur, D.; Kuriyan, J. Structural Insights into the Regulation of $Ca^{2+}$ /Calmodulin-Dependent Protein Kinase II (CaMKII). *Cold Spring Harb Perspect Biol* **2019**, a035147. https://doi.org/10.1101/cshperspect.a035147.
(117) Zhang, M.; Jang, H.; Gaponenko, V.; Nussinov, R. Phosphorylated Calmodulin Promotes PI3K Activation by Binding to the SH2 Domains. *Biophysical Journal* **2017**, *113* (9), 1956–1967. https://doi.org/10.1016/j.bpj.2017.09.008.
(118) Tian, J.; Zhang, X.; Wu, H.; Liu, C.; Li, Z.; Hu, X.; Su, S.; Wang, L.-F.; Qu, L. Blocking the PI3K/AKT Pathway Enhances Mammalian Reovirus Replication by Repressing IFN-Stimulated Genes. *Front. Microbiol.* **2015**, *6*. https://doi.org/10.3389/fmicb.2015.00886.
(119) Noyce, R. S.; Collins, S. E.; Mossman, K. L. Identification of a Novel Pathway Essential for the Immediate-Early, Interferon-Independent Antiviral Response to Enveloped Virions. *Journal of Virology* **2006**, *80* (1), 226–235. https://doi.org/10.1128/JVI.80.1.226-235.2006.

(120) Holm, C. K.; Jensen, S. B.; Jakobsen, M. R.; Cheshenko, N.; Horan, K. A.; Moeller, H. B.; Gonzalez-Dosal, R.; Rasmussen, S. B.; Christensen, M. H.; Yarovinsky, T. O.; Rixon, F. J.; Herold, B. C.; Fitzgerald, K. A.; Paludan, S. R. Virus-Cell Fusion as a Trigger of Innate Immunity Dependent on the Adaptor STING. *Nat Immunol* **2012**, *13* (8), 737–743. https://doi.org/10.1038/ni.2350.

(121) Mathavarajah, S.; Salsman, J.; Dellaire, G. An Emerging Role for Calcium Signalling in Innate and Autoimmunity via the CGAS-STING Axis. *Cytokine & Growth Factor Reviews* **2019**, S1359610119300383. https://doi.org/10.1016/j.cytogfr.2019.04.003.

(122) Shu, C.; Yi, G.; Watts, T.; Kao, C. C.; Li, P. Structure of STING Bound to Cyclic Di-GMP Reveals the Mechanism of Cyclic Dinucleotide Recognition by the Immune System. *Nat Struct Mol Biol* **2012**, *19* (7), 722–724. https://doi.org/10.1038/nsmb.2331.

(123) Lee, M. N.; Roy, M.; Ong, S.-E.; Mertins, P.; Villani, A.-C.; Li, W.; Dotiwala, F.; Sen, J.; Doench, J. G.; Orzalli, M. H.; Kramnik, I.; Knipe, D. M.; Lieberman, J.; Carr, S. A.; Hacohen, N. Identification of Regulators of the Innate Immune Response to Cytosolic DNA and Retroviral Infection by an Integrative Approach. *Nat Immunol* **2013**, *14* (2), 179–185. https://doi.org/10.1038/ni.2509.

(124) Mank, M.; Griesbeck, O. Genetically Encoded Calcium Indicators. *Chemical Reviews* **2008**, *108* (5), 1550–1564.

(125) Perry, J. L.; Ramachandran, N. K.; Utama, B.; Hyser, J. M. Use of Genetically-Encoded Calcium Indicators for Live Cell Calcium Imaging and Localization in Virus-Infected Cells. *Methods* **2015**, *90*, 28–38. https://doi.org/10.1016/j.ymeth.2015.09.004.

(126) Mukherjee, A.; Morosky, S. A.; Shen, L.; Weber, C. R.; Turner, J. R.; Kim, K. S.; Wang, T.; Coyne, C. B. Retinoic Acid-Induced Gene-1 (RIG-I) Associates with the Actin Cytoskeleton via Caspase Activation and Recruitment Domain-Dependent Interactions. *J. Biol. Chem.* **2009**, *284* (10), 6486–6494. https://doi.org/10.1074/jbc.M807547200.

(127) Ezelle, H.; Malathi, K.; Hassel, B. The Roles of RNase-L in Antimicrobial Immunity and the Cytoskeleton-Associated Innate Response. *IJMS* **2016**, *17* (1), 74. https://doi.org/10.3390/ijms17010074.

(128) Saxton, R. A.; Sabatini, D. M. MTOR Signaling in Growth, Metabolism, and Disease. *Cell* **2017**, *168* (6), 960–976. https://doi.org/10.1016/j.cell.2017.02.004.

(129) Cao, W.; Manicassamy, S.; Tang, H.; Kasturi, S. P.; Pirani, A.; Murthy, N.; Pulendran, B. Toll-like Receptor-Mediated Induction of Type I Interferon in Plasmacytoid Dendritic Cells Requires the Rapamycin-Sensitive PI(3)K-MTOR-P70S6K Pathway. *Nat Immunol* **2008**, *9* (10), 1157–1164. https://doi.org/10.1038/ni.1645.